AD_____

Award Number: DAMD17-99-1-9002

TITLE: Characterization of Putative Homeostatic Molecules in Prostate Development and Androgen-Independent Prostate Cancer

PRINCIPAL INVESTIGATOR: Jer-Tsong Hsieh, Ph.D.

CONTRACTING ORGANIZATION: The University of Texas Southwestern Medical Center at Dallas
Dallas, Texas 75390-9105

REPORT DATE: January 2001

TYPE OF REPORT: Annual

PREPARED FOR: U.S. Army Medical Research and Materiel Command
Fort Detrick, Maryland 21702-5012

REPORT DOCUMENTATION PAGE

Form Approved
OMB No. 074-0188

1. AGENCY USE ONLY (Leave blank)	2. REPORT DATE	3. REPORT TYPE AND DATES COVERED
	January 2001	Annual (1 Jan 00 - 31 Dec 00)

4. TITLE AND SUBTITLE:
Characterization of Putative Homeostatic Molecules in Prostate Development and Androgen-Independent Prostate Cancer

5. FUNDING NUMBERS
DAMD17-99-1-9002

6. AUTHOR(S)
Jer-Tsong Hsieh, Ph.D.

7. PERFORMING ORGANIZATION NAME(S) AND ADDRESS(ES)
The University of Texas Southwestern Medical Center
at Dallas
Dallas, Texas 75390-9105
E-Mail: JT.Hsieh@Utsothwestern.edu

8. PERFORMING ORGANIZATION REPORT NUMBER

9. SPONSORING / MONITORING AGENCY NAME(S) AND ADDRESS(ES)
U.S. Army Medical Research and Materiel Command
Fort Detrick, Maryland 21702-5012

10. SPONSORING / MONITORING AGENCY REPORT NUMBER

11. SUPPLEMENTARY NOTES

12a. DISTRIBUTION / AVAILABILITY STATEMENT
Approved for Public Release; Distribution Unlimited

12b. DISTRIBUTION CODE

13. ABSTRACT ***(Maximum 200 Words)***

Androgen-independent (AI) prostate cancer (PCa) is a life-threatening disease. No effective treatment is available for this disease because the biology of AIPCa is still unknown. It is known that AIPCa possesses many similar properties of the basal (or stem) cell in prostate. Therefore, in this project, we studied the signal pathway(s) controlling growth/differentiation of basal cells of prostate. We focused on two unique molecules, C-CAM1 and DOC-2, because both proteins often loss their expression on PCa and are a potent growth inhibitor.

For C-CAM1, we analyzed the functional domain of C-CAM1 that modulates its tumor suppression function. We found that Ser/Thr phosphorylation site but not in the tyrosine phosphorylation site of C-CAM1 resulted in the loss of tumor suppressive activity. These data indicate that the potential Ser/Thr phosphorylation site in the intracellular domain of the C-CAM molecule is crucial for the suppression of the growth of PCa.

For DOC-2, we recently demonstrated that the N-terminus of DOC-2 can interact with a novel Ras-GAP protein that can inactivate Ras-mediated gene expression. Also, the C-terminus of DOC-2 is able to sequester Grb2, a key effector protein involved in protein receptor tyrosine kinase-mediated MAP kinase activation, which results in the inhibition of MAP kinase activation.

Taken together, our data indicate that both C-CAM1 and DOC-2 act as homeostatic factor to modulate mitogen signaling in normal basal cell. Down regulation of these factors may render PCa acquire its AI status.

14. SUBJECT TERMS	15. NUMBER OF PAGES
stem cell, androgen-independent growth, tumor suppressor, adaptor protein, cell adhesion molecule, prostate cancer	71
	16. PRICE CODE

17. SECURITY CLASSIFICATION OF REPORT	18. SECURITY CLASSIFICATION OF THIS PAGE	19. SECURITY CLASSIFICATION OF ABSTRACT	20. LIMITATION OF ABSTRACT
Unclassified	Unclassified	Unclassified	Unlimited

Table of Contents

INTRODUCTION

The purpose of this study is to define the signaling pathways that control growth and differentiation of prostatic epithelia. Homeostatic factor(s) that operate in the androgen-independent (AI) basal cell population of the prostate can modulate the stimuli for extracellular growth by regulating particular gene(s) expressed in the nucleus. Genes with a potent growth inhibitory effect on prostate cancer, C-CAM1 and DOC-2, were chosen for the study because C-CAM1 behaves like a membrane receptor and DOC-2 is a signaling molecule. Moreover, both are novel genes, which have recently been reported by this laboratory. To delineate the signaling network elicited by these genes, three aims were proposed: 1) to specify the interaction of C-CAM1 and DOC-2 during development of the prostate and of carcinogenesis; 2) to identify the signaling pathway elicited by these putative homeostatic molecules; and 3) to document the effect of microenvironment factors on the regulation of these molecules. Recurrent AI prostate cancer (PCa) has been shown to possess many similar characteristics with the population of AI basal cells in the normal prostate. With the support of Department of Defense, our project has generated many new reagents available for research community, discovered new gene, and unveiled new pathway to modulate cell growth and differentiation of prostatic epithelia. We have published two peer-review papers, two abstracts, and one manuscript in submission. The outcome of this study can help us to understand the biology of normal basal (or stem) cell in prostate and plan new treatment strategy for AIPCa cells.

BODY

Task 1. To specify the interaction of C-CAM1 and DOC-2 during development of the prostate and of carcinogenesis.

Recently, we demonstrated that expression of C-CAM1, an immunoglobulin (Ig)-like CAM, correlates with androgen-induced prostate epithelial differentiation in an organ-specific manner (1). Constitutive expression of the C-CAM protein was detected in normal prostatic epithelium throughout the fetal to adulthood stage (2). However, C-CAM expression was diminished in both prostate intraepithelial neoplasia and cancer lesions (2), which indicates that loss of C-CAM expression may be involved in the early stages of prostate carcinogenesis. In addition, increased C-CAM expression, through gene transfection or delivery of recombinant adenovirus, can effectively control growth of prostate cancer both *in vitro* (3) and *in vivo* (4). According to sequence analysis of C-CAM1 cDNA, C-CAM1 represents a unique CAM with a potential signal transducing capability. Therefore, the relationship of each C-CAM structural domain that could possibly affect its tumor suppression function *in vivo* was analyzed using a variety of mutants – ranging from deletion mutation of the extracellular domain to the intracellular domain. Because of its high infectivity, an adenoviral vector system was employed as a delivery system. Data from *in vivo* tumorgenic assay indicated that the C-CAM mutant without cell adhesion function retained its tumor suppressive activity. In contrast, deletion in the Ser/Thr phosphorylation site but not in the tyrosine phosphorylation site of C-CAM1 resulted in the loss of tumor suppressive activity. These data suggest that, in contrast to the extracellular domain, the potential Ser/Thr phosphorylation site in the intracellular domain of the C-CAM molecule and its associated protein(s) are crucial for the suppression of the growth of prostate cancer (Appendix 1).

Elevated levels of DOC-2 mRNA and protein are detected in the degenerated prostate (5). Immunohistochemical staining indicates that both DOC-2 and C-CAM1 proteins are associated with the enriched basal cells in the prostate (1, 5). Furthermore, restored expression of DOC-2 can inhibit the growth of prostate cancer (5). It is likely that both proteins have an interaction. So, to further delineate the possible interaction between DOC-2 and C-CAM1, a co-immunoprecipitation experiment was conducted by transfecting both DOC-2 and C-CAM1 expression vectors. As shown in Fig. 1, no physical interaction between these proteins can be detected. This suggests that DOC-2 and C-CAM1 proteins may not contact directly.

Fig. 1 The possible interaction between DOC-2 and C-CAM1. Cells were co-transfected with DOC-2 plus either DIP1/2 or C-CAM1 expression vectors for 48 h, then cell lysate were immunoprecipitated with primary antibody, then immunocomplex was subjected to western blotting. **1**, cells were co-transfected with both DOC-2 and DIP1/2 vectors. **2**, cells were co-transfected with both DOC-2, and C-CAM1 vectors. IP: immunoprecipitation. WB, western blotting.

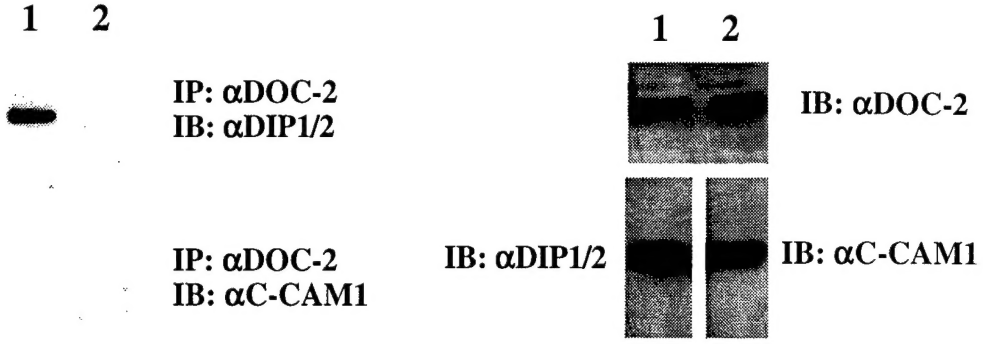

Task 2. To identify the signaling pathway elicited by these putative homeostatic molecules.

Our previous data demonstrated that the presence of an unknown factor(s) was associated with DOC-2 protein by immunoprecipitation. We used a yeast two-hybrid system (6) to search for these factors. Initially, the bait vector was constructed from pVJL11 by inserting the N-terminus of DOC-2 protein (i.e., residues 1-269), which had been demonstrated to the major protein phosphorylation site in DOC-2. Among an estimated $9X10^4$ clones plated for screening, 94 clones with His^+ phenotype were obtained. But, only 34 clones appeared positive in both His and LacZ phenotypes. After screening with mating test to rule out false positive results, 3 independent clones, DIP1 (1.7 kb), DIP2 (5.5 kb), and DIP7 (2.8 kb) were confirmed. Further cDNA sequencing and alignment (Appendix 2) suggest these clones belong to, and are novel members of, the GTPase activating protein (i.e., GAP) family. The sequence alignment data also suggests that these clones share some homologue with the C-terminus of the GAP sequence that is known to interact with RAS-protein (7). The DIP1 and DIP2 sequences overlapped, which indicates that both derive from the same cDNA species.

To unveil their expression pattern in different tissues and organs, and to demonstrate each clone's distinct pattern, northern analysis (Appendix 2) was performed. For example, DIP7, with a major 6.0 kb transcript, appears to be brain-specific, while DIP1 and DIP2, with at least two transcripts (7.0 kb and 4.7 kb), appear present in brain, kidney, and both prostatic epithelial and stromal cell cultures. This suggests that at least two groups of DIPs are present in brain and other tissues. Interestingly, DIP1/2 was detected in prostatic epithelial cells derived from the basal cells (e.g., NbE and VPE), but it was not detected in intact VP because the basal cell population constitutes only 5% of the total prostatic epithelia in intact VP.

After screening another brain cDNA library, we cloned a full-length cDNA of DIP1/2. The deduced sequence of a full-length DIP1/2 (Appendix 2) indicated that an open reading of 996 amino acids contains three unique domain: a GAP domain (aa 194-409), a proline-rich domain (aa 727-736), and a leucine zipper domain (aa 842-861). Using synthetic peptide derived from the C-terminus of DIP1/2, we raised a polyclonal antibody specific against DIP1/2 (Appendix 2). In contrast to preimmune serum, the polyclonal antibody can specifically recognize a 130 kD protein derived from *in vitro* translation of DIP1/2 cDNA. In the rat brain we observed several additional protein bands that may be produced by protein modification and/or isoform. The polyclonal antibody should be a specific antibody against DIP1/2.

To characterize the biochemical properties of DIP1/2, we demonstrated that DIP1/2 has RAS-GAP activity *in vitro* and *in vivo*. Since RAS protein functions as an essential component in many intracellular signaling pathways responsible for differentiation, proliferation, and apoptosis. The Raf-MEK-ERK pathway is a key signal transduction pathway modulated by RAS protein. We demonstrated that DIP1/2 alone protein is able to inhibit this cascade. The interaction between DOC-2 and DIP1/2 further enhance the GAP activity of DIP1/2 (Appendix 2).

Previously we demonstrate that PKC-elicited DOC-2/DAB2 phosphorylation can block TPA-induced gene activity (8). Therefore, we investigated whether DIP1/2 is a mediator involved in this action. We found that ΔB (C-terminal deletion mutant of DOC-2) or DIP1/2 alone was able to inhibit TPA-induced TRE reporter gene activity (Appendix 2). Conversely, combing ΔB-S24A mutant with DIP1/2 failed to have any inhibitory effect because S^{24A} in DOC-2/DAB2 is the key amino acid to modulate this activity. We observed an additive effect on inhibiting TRE reporter gene activity in the presence of ΔB and DIP1/2. In contrast, ΔB-S24A and DIP1/2 did not have any additive effect. These data indicated that S24 phosphorylation in DOC-2 enhanced the binding to the DIP1/2 in prostatic epithelia.

Because DIP1/2 appears to be a negative regulator for the RAS-mediated pathway, it may function as a growth inhibitor. To test this, C4-2 cells (a tumorgenic human prostate cancer cell line) were transfected with a DIP1/2 expression vector. Initially, we observed that there were fewer surviving clones in the DIP1/2-transfected plate than in plasmid control-transfected cells despite the same number of cells being used in transfection. We found the growth rate of DIP1/2-transfected cells was significantly lower than the control cell (Appendix 2). Furthermore, using transient transfection method, we demonstrated that an elevated DIP1/2 expression resulted in less colony formation in C4-2 cells (Appendix 2). These data indicate that DIP1/2's GAP activity modulates its growth inhibitory effect. DIP1/2 appears to be a potent growth inhibitor for prostate cancer.

Task 3. The impact of microenvironment factors on the regulation of these putative homeostatic molecules.

To determine the possible impact of microenvironment factors (such as EGF, NT3) on regulating the activity of DOC-2, we decide to investigate the role of DOC-2 in EGF-induced signal pathway. In our recent publication (Appendix 3), we demonstrated that increased *in vitro* binding of DOC-2 to Grb2 can be detected in a time dependent manner in C4-2 cells treated by EGF or in PC12 cells treated by NT3. On the other hand, we used co-immunoprecipitation to confirm the intracellular interaction between DOC-2 and Grb2. Data from both Grb2 binding assay and co-IP assay indicated that the interaction between DOC-2/DAB2 and Grb2 was enhanced under the stimulation of peptide growth factors. We further investigated the status of down stream effector protein (e.g., Erk kinase) and gene transcription. The presence of DOC-2 was able to inhibit Erk kinase phosphorylation (active Erk) and SRE reporter gene transcription. Taken together, we believe that DOC-2 is a potent inhibitor for RPTK-mediated signal cascade.

To delineate the underlying mechanism for this inhibitory effect, we demonstrated the C-terminus of DOC-2 (i.e., ΔN) responsible for the binding to Grb2 protein. Structurally, the C-terminus of DOC-2 contains three proline-rich domains. To further compare the binding affinity of these proline-rich sequences, four oligopeptides were synthesized based on DOC-2/DAB2 protein sequence: PPQ (aa 619-627); PPL (aa 663-671); LLL (aa 663-671 with all proline residues substituted with leucine residues) and PPK (aa 714-722). Using these peptides, we demonstrated that the second proline-rich domain is the major interactive site with Grb2 and proline is the key amino acid residue. It is known that the interaction between Grb2 protein and the activated receptor can initiate the translocation of a group of proteins, Guanine Nucleotide Exchange Factors (such as SOS), which activates RAS activity. We were able to show that increased expression of p82 levels suppresses the binding of Grb2 to SOS, indicating that both DOC-2 and SOS are competing with the same SH3 site in Grb2 (Appendix 3). We further showed that PPL but not LLL is able to neutralize the inhibitory effect of DOC-2 on Erk phosphorylation in NbE (rat normal prostatic epithelial line) expressing endogenous DOC-2 and gene transcription in C4-2 cells.

These data clearly indicate that the C-terminus of DOC-2 competes with SOS for Grb2 binding that leads to the inactivation of RPTK-mediated signal transduction. Furthermore, we also found that the C-terminus of DOC-2 was able to interact with several SH3-containing proteins (Fig. 2). These data suggest that DOC-2 complex may play a key role in modulating peptide growth factors-induced signal transduction.

Fig. 2 Determination of interaction domain between DOC-2/DAB2 and SH3 containing protein. A rapid screening for the interaction between DOC-2 and SH3 containing proteins by pull down experiment (Appendix 3).

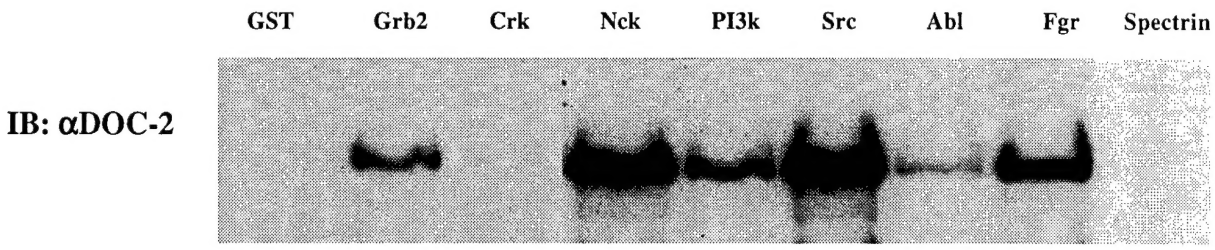

KEY RESEARCH ACCOMPLISHMENT

- Dissociated the Ig domain (for adhesion activity) of the C-CAM1 protein with its tumor suppression activity.
- Determined the functional domain of the C-CAM1 protein (i.e., intracellular domain) for its tumor suppression activity.
- Identified a novel gene (i.e., DIP1/2) from RAS-GAP family as an effector protein interacting with the N-terminus of DOC-2 protein.
- Cloned a full-length DIP1/2 cDNA and generated a specific antibody for DIP1/2 protein.
- Demonstrated the presence of DIP1/2 in normal epithelial culture cells derived from basal cell of the rat prostate and the loss of DIP1/2 expression in AIPCa cell lines.
- Demonstrated the RAS-GAP activity of DIP1/2 can be enhanced via binding with DOC-2 protein.
- Demonstrated DIP1/2 as a potent growth inhibitor in PCa cell lines.
- Determined a specific interaction of Grb2 proteins with the C-terminus of DOC-2 proteins.
- Microenvironment factors such as EGF, NT3 enhanced the binding between Grb2 and the C-terminus of DOC-2 proteins.
- The binding between Grb2 and DOC-2 disabled the Grb2-mediated MAP kinase activation.
- Demonstrated the protein complex of DOC-2 functioning a unique negative regulatory in prostatic epithelia.

REPORTABLE OUTCOMES

FULL-LENGTH PAPER

1. Hsieh, J.T., Early K, Pong, R.C., Wang, Y., Van, N.T., and Lin S-H. (1999) Structural analysis of C-CAM1 molecule for its tumor suppression function in prostate cancer cells. Prostate, 41, 31-38.

2. Wang, Z., Tseng, C-P., Pong, R-C., McConnell, J.D., and Hsieh, J.T. (2001) A Novel RasGTPase activating protein that interacts with DOC-2/DAB2: A downstream effector leading to the suppression of prostate cancer. J. Biol. Chem., (submitted).

3. Zhou, J., and Hsieh, J.T. (2001) The inhibitory role of DOC-2/DAB2 in growth factor receptors mediated signal cascade: DOC-2/DAB2-mediated inhibition of Erk phosphorylation via binding to Grb2. J. Biol. Chem., 278, 27793-27798.

ABSTRACT

1. Tseng, C.P., Wang, Z., Pong, R.C., Li, Y., Ely, B., and Hsieh, J.T. (1999) An underlying mechanism of tumor suppressor gene, DOC-2, in prostate cancer. J. Urol., 160, 60A.

2. Wang, Z., Tseng, C-P., Pong, R.C., Sherif, H., and Hsieh, J.T. (2000) A novel signaling pathway in prostate development and cancer progression. J. Urol., 163, 30A.

PERSONNEL

Li, Yingming, M.B. (research assistant)

Zhou, Jian, Ph.D. (postdoctoral fellow)

Wang, Zhi, Ph.D. (postdoctoral fellow)

Scholes, Jessica, B.S. (research assistant)

CONCLUSIONS

The prostate gland is an exquisitely androgen-dependent organ, in particular, the prostatic epithelium. The lamina epithelium requires androgen for maintaining its cell architecture and normal physiologic function; it undergoes apoptosis with androgen deprivation. In contrast, the basal epithelium, an androgen-independent cell population, remains in the degenerated gland and can fully regenerate the entire gland back to normal preprogrammed size in the presence of androgen. Therefore, the basal cell population may represent a stem cell population and homeostatic signal(s) in stem cells may play a critical role in controlling growth/differentiation of prostate gland. However, the biochemical and molecular characterization of prostatic stem cells are not well defined. The basal cells of the prostate gland, considered as a stem cell population, are not only responsible for maintaining homeostasis of the normal prostate but also contribute to the progression of AI prostate cancer. Until now, the regulatory pathway(s) involved in prostate homeostasis was undefined. In this study we have examined: 1) the functional role of two unique basal cell-associated genes, C-CAM1 and DOC-2, in AI prostate cancer, and 2) the signaling network elicited by these two genes.

We were able to define the intracellular domain containing a Ser/Thr phosphorylation site as a key domain to modulate the tumor suppression function of the C-CAM1 protein (Appendix 1). Our results clearly indicate that the C-CAM1 protein can function like a membrane receptor in order to initiate a cascade of phosphorylation events through a variety of adapter proteins and kinases, which subsequently culminate in a wave of immediate early gene expression in the nucleus. Therefore, because we have ruled out any possible interaction between C-CAM1 and DOC-2 proteins, the immediate study is to identify the effector protein(s) associated with DOC-2 protein.

We have shown that DOC-2 can suppress the *in vitro* growth of PCa cells (5). In our recent study, we demonstrated that phosphorylation of serine 24 in the N-terminus of the DOC-2 protein correlates with its activity (6). Using the yeast two-hybrid screening system we identified a novel gene, DIP1/2, belonging to the RAS-GAP family, as an immediate interactive protein for DOC-2. DIP1/2 appears to express in many tissues, including degenerated prostates and prostatic epithelial cell cultures derived from the basal cell population. Further characterization of DIP1/2 indicated that GAP activity of DIP1/2 can be enhanced in the presence of DOC-2 and DIP1/2 and DOC-2 has an additive effect on the growth inhibition of PCa cells. Therefore, we believe DIP1/2 is one of key mediator for DOC-2-elicited signal transduction.

Moreover, we also characterized the effect of microenvironment factor (such as peptide growth factors) on the DOC-2's activity. In this study, we demonstrated that peptide growth factors-induced signal transduction can be inhibited in the presence of DOC-2. This was due to that the C-terminus of DOC-2 was able to sequester Grb2 that can recruit SOS for RAS activation. In addition to Grb2 binding, the proline-rich domain in the C-terminus of DOC-2 was able to other SH3-containing protein. Taken together, we believe DOC-2 protein complex play a critical role in maintaining the homeostasis of prostatic epithelia.

This study signifies the potential role of homeostatic factors in the progression of PCa. These new molecules may serves as surrogate markers for predicting the biologic behavior of PCa. Moreover, the information gleaned from this study can be used to formulate a new regimen able to intervene sooner during the multiple steps of prostate carcinogenesis.

REFERENCES

1. Hsieh, J.T., and Lin S-H., (1994) Androgen regulation of cell adhesion molecule (CAM) gene expression in rat prostate during organ degeneration: C-CAM belongs to a new class of androgen-repressed genes associated with enriched stem/amplifying cell population after prolonged castration. J. Biol. Chem., 269, 3711-3716.

2. Kleinerman, D., Troncoso, P., Lin S-H., Pisters L.L., Sherwood E.R., Brooks T., von Eschenbach A.C., and Hsieh, J.T. (1995) Consistent expression of an epithelial cell adhesion molecule (C-CAM) during human prostate development and loss of expression in prostate cancer: implication as a tumor suppressor. Cancer Res., 55, 1215-1220.

3. Hsieh, J.T., Luo, W., Song, W., Wang, Y., Kleinerman, D., Van, N.T., and Lin S-H. (1995) Tumor suppressive role of an androgen-regulated epithelial cell adhesion molecule (C-CAM) in prostate carcinoma cell revealed by sense and antisense approaches. Cancer Res., 55, 190-197.

4. Kleinerman, D., Zhang, W.W., von Eschenbach, A.C., Lin S-H., and Hsieh, J.T. (1995) Application of a tumor suppressor gene, C-CAM1, in androgen-independent prostate cancer therapy: a preclinical study. Cancer Res., 55, 2831-2836.

5. Tseng, C-P., Ely, B., Pong, R-C., Li, Y., and Hsieh, J.T. (1998) Regulation of the DOC-2 gene during castration-induced rat ventral prostate degeneration and its growth inhibitory function in human prostatic carcinoma cells. Endocrinology, 139, 3542-3553.

6. Chien, C.T. Bartel, P.L., Sternglanz R., and Fields, S. (1991) The yeast two-hybrid system: A Method to identify any clone genes for proteins that interact with a protein of interest. Proc. Natl. Acad. Sci., 88: 9578-9582.

7. Ahmadian, M.R., Wiesmuller, L., Lautwein, A., Bischoff, F.R., and Wittinghofer (1996) Structural differences in the minimal catalytic domain of the GTPase-activating proteins $p120^{GAP}$ and Neurofibomin. J. Biol. Chem., 271, 16409-16415.

8. Tseng, C-P., Ely, B., Pong, R-C., Li, Y., Wang, Z., Zhou, J., and Hsieh, J.T. (1999) The role of DOC-2/Dab2 protein phosphorylation in the inhibition of AP-1 activity-an underlying mechanism of its tumor suppressive function. J. Biol. Chem., 274, 31981-31986.

APPENDICES

1. Hsieh, J.T., Early K, Pong, R.C., Wang, Y., Van, N.T., and Lin S-H. (1999) Structural analysis of C-CAM1 molecule for its tumor suppression function in prostate cancer cells. Prostate, 41, 31-38.

2. Wang, Z., Tseng, C-P., Pong, R-C., McConnell, J.D., and Hsieh, J.T. (2001) A Novel RasGTPase activating protein that interacts with DOC-2/DAB2: A downstream effector leading to the suppression of prostate cancer. J. Biol. Chem., (submitted).

3. Zhou, J., and Hsieh, J.T. (2001) The inhibitory role of DOC-2/DAB2 in growth factor receptors mediated signal cascade: DOC-2/DAB2-mediated inhibition of Erk phosphorylation via binding to Grb2. J. Biol. Chem., 278, 27793-27798.

The Prostate 41:31–38 (1999)

Appendix 1

Structural Analysis of the C-CAM1 Molecule for Its Tumor Suppression Function in Human Prostate Cancer

Jer-Tsong Hsieh,[1]* Karen Earley,[2] Rey-Chen Pong,[1] Yan Wang,[2] Nguyen T. Van,[3] and Sue-Hwa Lin[2]

[1]*Department of Urology, University of Texas Southwestern Medical Center, Dallas, Texas*
[2]*Department of Molecular Pathology, University of Texas M.D. Anderson Cancer Center, Houston, Texas*
[3]*Department of Hematology, University of Texas M.D. Anderson Cancer Center, Houston, Texas*

BACKGROUND. Recently, we demonstrated that expression of C-CAM1, an immunoglobulin (Ig)-like cell adhesion molecule (CAM), was diminished in both prostate intraepithelial neoplasia and cancer lesions, indicating that loss of C-CAM1 expression may be involved in the early events of prostate carcinogenesis. Also, increased C-CAM1 expression can effectively inhibit the growth of prostate cancer. Structurally, C-CAM1 represents a unique CAM with a potential signal transducing capability. In this study, we further analyzed the functional domain of C-CAM1 for controlling its tumor suppression function.

METHODS. Recombinant adenoviruses expressing a series of C-CAM1 mutants were generated, such as AdCAMF488 (mutated C-CAM1 containing Tyr-488 → Phe-488), AdCAMH458 (intracellular domain deletion mutant containing 458 amino acids), AdCAMG454 (intracellular domain deletion mutant containing 454 amino acids), and AdCAMΔD1(C-CAM1 mutant containing first Ig domain deletion). After in vitro characterization of each virus, human prostate cancer cells infected with these viruses were subcutaneously injected into athymic mouse. Both tumor incidence and volume were measured for determining the tumor suppression function for each mutant.

RESULTS. In vivo tumorigenic assay indicated that AdCAMΔD1 without cell adhesion function still retained its tumor suppression activity. In contrast, both AdCAMH458 and AdCAMG454 decreased or lost their tumor suppression activity.

CONCLUSIONS. Our data indicate that the intracellular domain of the C-CAM1 molecule is critical for inhibiting the growth of prostate cancer, suggesting that C-CAM1 interactive protein(s) may dictate prostate carcinogenesis. *Prostate 41:31–38, 1999.*

KEY WORDS: **cell adhesion molecule; tumor suppressor; prostate cancer**

INTRODUCTION

In multicellular organisms, ontogenesis is orchestrated by cell-cell interactions among different cell types throughout embryogenesis. Cell adhesion molecules (CAMs) play a central role in coordinating the entire process. Very often, altered CAM expression results in changing the homeostasis of normal cells and leads to hyperplastic growth of cells. In recent

Abbreviations: CAM, cell adhesion molecule; FACS, fluorescence-activated cell sorting; FBS, fetal bovine serum; FITC, fluorescein isothiocyanate; Ig, immunoglobulin; kb, kilobase; kDa, kilodalton.

Grant sponsor: National Institutes of Health; Grant number: CA 59939. Grant sponsor: U.S. Army; Grant number: PC 970259.

*Correspondence to: Dr. Jer-Tsong Hsieh, Department of Urology, University of Texas Southwestern Medical Center, 5323 Harry Hines Blvd., Dallas, TX 75235. E-mail: Hsieh@utsw.swmed.edu

Received 23 December 1998; Accepted 22 April 1999

studies, we demonstrated that an androgen-repressed CAM [1], C-CAM1, was inversely correlated with the status of premalignant lesions of human prostate cancer, i.e., prostate intraepithelial neoplasia, and cancer lesions as well, indicating that C-CAM1 may be a potent tumor suppressor in prostate carcinogenesis [2]. To demonstrate the tumor-suppressive function of C-CAM1, we transfected a high-tumorigenic prostate cancer line (PC-3) with a C-CAM1 expression vector [3], or infected PC-3 cells with a recombinant adenovirus expressing C-CAM1 cDNA [4]. In both cases, both the in vitro and in vivo growth of prostate cancer cells was significantly inhibited. In addition, by decreasing endogenous expression of C-CAM levels in a nontumorigenic prostatic epithelium cell line with an antisense vector resulted in an increase of the in vivo tumorigenicity of this cell line [3]. Therefore, C-CAM is a potent tumor suppressor in human prostate cancer.

Based on cDNA sequences, the structure of the C-CAM1 molecule is very similar to that of the carcinoembryonic antigen (CEA) and belongs to the immunoglobulin (Ig) gene superfamily. However, C-CAM1 represents a new family of Ca^{2+}-independent CAMs because it contains three distinct domains, i.e., the extracellular, the transmembrane, and intracellular domains. The first Ig loop in the extracelluar domain is critical for the intercellular adhesion of C-CAM1 [5]. Also, the transmembrane domain is required for C-CAM1 as a cell surface molecule. Interestingly, the cytoplasmic (or intracellular) domain with 71 amino acids contains at least two potential phosphorylation sites, including one for cAMP-dependent kinase and tyrosine kinase, suggesting that C-CAM1 may function as a receptor to initiate a signaling pathway. However, the functional domain(s) of C-CAM1 as a tumor suppressor in prostate cancer is still unknown. Therefore, we decided to analyze the effect of each domain of the C-CAM1 molecule on the in vivo growth inhibition of prostate cancer.

MATERIALS AND METHODS

Construction and Characterization of Recombinant Adenoviruses Containing C-CAM Deletion Mutants

To generate recombinant adenoviruses containing various deletion mutants of C-CAM1 cDNA, the cDNAs were directionally cloned into the *Hind*III and *Not*I sites of a shuttle vector (pAdE1CMV/pA) and cotransfected with the pJM17 vector into 293 cells, as described previously [4]. After a large-scale production using two cycles of CsCl ultracentrifugation, the titer of each virus was determined by the plaque assay as follows: AdCAM101 (3.4×10^{10} pfu/ml); AdCAM902 (1.1×10^{10} pfu/ml); AdCAMΔD1 (1.8×10^{10} pfu/ml); AdCAMF488 (4.0×10^{10} pfu/ml); AdCAMG454 (3.9×10^{10} pfu/ml); and AdCAMH458 (1.3×10^{10} pfu/ml).

In this study, we used both adenoviral DNA and viral infectivity to characterize each recombinant adenovirus. To confirm the presence of the cDNA insert, recombinant adenoviral genomic structure was carried out using the polymerase chain reaction (PCR), as described previously [4]. In the PCR reaction, three sets of primer were used separately: primer set B [6] was used for identifying the presence of the cDNA insert; primer set C [6] was used for identifying the presence of viral sequences; primer set D [$^{5'}$ATTACCGAAGAAATGGCCGC$^{3'}$, $^{5'}$CCCATTTAACACGCCATGCA$^{3'}$] [7] was used for examining the presence of the E1 region. On the other hand, viral infectivity was determined in the PC-3 cells 24 hr after viral infection by fluorescent-activated cell scanning (FACS) analysis, as described previously [4].

Determination of Viral Infectivity of PC-3 Cells by Fluorescent-Activated Cell Scanning Analysis

PC-3 cells were infected with different viruses at 100 m.o.i. (multiplicity of infection) and incubated at 37°C for 24 hr. Immunofluorescence staining was carried out as described previously [4], and then the percentage of positive cells was determined by a dual-laser Vantage flow cytometer (Becton Dickinson, Mountain View, CA).

Determination of C-CAM1 Expression and Cell Adhesion Activity in PC-3 Cells by C-CAM Recombinant Adenoviruses

To determine the levels of C-CAM1 expression in viral-infected cells, we performed both Northern and Western blot assays, as described previously [1]. In Northern blot analysis, a radiolabeled C-CAM cDNA fragment generated from *Bam*HI and *Pst*I digestion was used for probing. For determining C-CAM1 protein expression by each clone, cells were infected with virus at 10 m.o.i. for 24 hr. The cell lysate was subjected to Western blot analysis using the antibody specific against C-CAM1 [8,9].

Cell adhesion activity in PC-3 cells after adenoviral infection was carried out for determining the function of the C-CAM molecule. One million PC-3 cells were resuspended in a 1.0-ml medium and mixed gently at room temperature to allow formation of cell aggregation. At any given time, cell adhesion activity was determined reciprocally by the presence of the percentage of single cells counted by a hemacytometer [3].

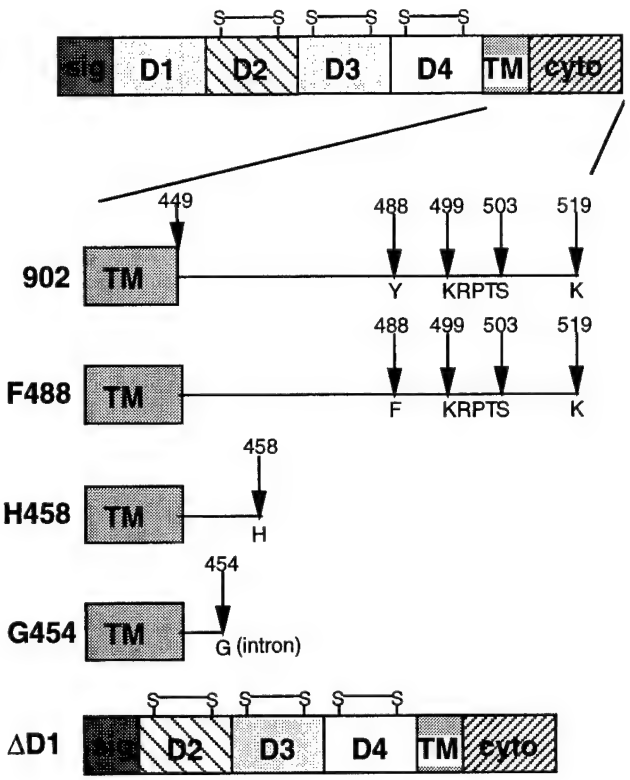

Fig. 1. Scheme of C-CAM1 structure and its deletion mutants. sig, signal peptide; D1, first Ig domain; D2, second Ig domain; D3, third Ig domain; D4, fourth Ig domain; TM, transmembrane domain; cyto, cytoplasmic domain. Y, tyrosine; K, Lysine; R, arginine; P, proline; T, threomine; S, servine; H, histidine; G, glycine; F, phenylalanine.

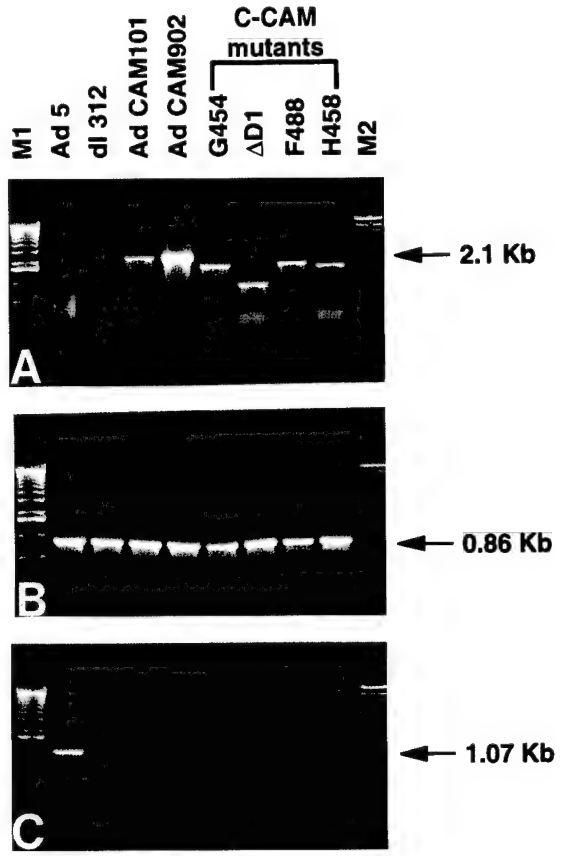

Fig. 2. Characterization of recombinant adenoviruses carrying the various C-CAM1 constructs. Recombinant adenoviruses carrying the different C-CAM1 deletion constructs were generated from homologous recombination, as described previously [4]. The PCR reaction was carried out for determining the genomic structure of each virus with three different sets of primers: primer set B (**A**), primer set C (**B**), and primer set D (**C**).

Assessment of In Vivo Tumorigenicity of PC-3 Cells

After viral infection for 18 hr, PC-3 cells were trypsinized, and cell numbers were counted by hemacytometer. One million cells were concentrated in a 100-μl volume and injected subcutaneously at six sites in the flanks of 8–10-week-old male nude mice. Tumors became palpable in about 1 month; the change in tumor volume was measured by a caliper and calculated using the formula described previously [3].

RESULTS

Generation and Characterization of the Recombinant Adenoviruses Carrying Various C-CAM1 Inserts

To assess the functional domain of C-CAM1 in suppressing tumor growth of human prostate cancer cells, we decided to create a variety of C-CAM1 mutants by altering the potential phosphorylation site or the deleting intracellular domain of the C-CAM1 molecule. As shown in Figure 1, a single base mutation on Tyr-488 of C-CAM1 was changed to phenylalanine with site-directed mutagenesis PCR, as described previously [10]. In addition, we deleted most of the amino acids in the intracellular domain to the His-458 position (i.e., AdCAMH458), or removed an additional four amino acids containing a potential Ser/The phosphorylation site to the Gly-454 position (i.e., AdCAMG454). On the other hand, the first Ig domain of C-CAM1 is known to play an important role in cell adhesion function [8]; therefore, a C-CAM1 mutant containing the first Ig domain deletion (i.e., AdCAMΔD1) was created to eliminate its cell adhesion function. Furthermore, two recombinant adenoviruses from a previous study [4], one containing a sense strand of C-CAM1 cDNA (i.e., AdCAM902) and the other containing an antisense strand of C-CAM1 cDNA (i.e., AdCAM101), were used in this study.

We performed a PCR reaction to determine the presence of an individual C-CAM1 insert from each adenovirus. As shown in Figure 2A, the size of each

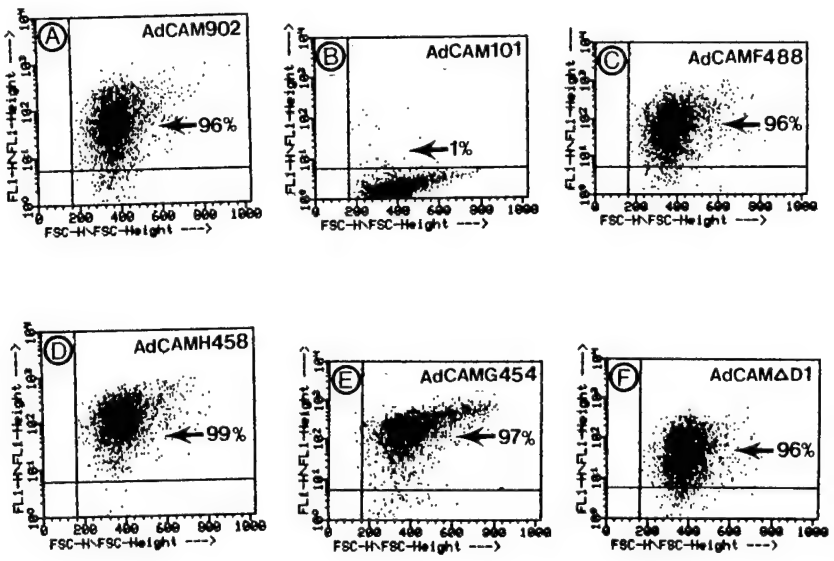

Fig. 3. Efficiency of infection by various C-CAM1 mutant adenoviruses in PC-3 cells determined by flow cytometry. Cells were infected with different C-CAM1 mutant adenoviruses (100 m.o.i.) for 24 hr and were then subjected to fluorescent-activated cell scanning analysis, using immunofluorescence staining. The dual-parameter histogram represents relative cell size (x-axis) measured from forward light scatters (FSC), and log of C-CAM1 expression levels (y-axis) measured from the green fluorescence intensity emitted by FITC-stained cells. Positive staining was defined as staining intensity greater than 10 FITC units, which was the background level from control cells stained with antibodies. Numbers in each graph indicate the percentage of positive cells infected by each virus. **A:** AdCAM902. **B:** AdCAM101. **C:** AdCAMF488. **D:** AdCAMH458. **E:** AdCAMG454. **F:** AdCAMΔD1.

PCR product corresponded to that of the individual C-CAM1 mutant. In addition, using a virus-specific primer set (Fig. 2B), we were able to confirm the presence of viral DNA from each recombinant virus. Furthermore, to rule out any possible contamination from wild-type adenovirus in each preparation, we employed a PCR reaction to determine the presence of E1 sequences in each C-CAM1 adenovirus, using the E1-specific primer set. The data in Figure 2C indicate that a 1.07-kb specific band was only detected in the wild-type adenovirus (i.e., Ad5), and not in C-CAM1 viruses and other control viruses such as dl312 with an E1-deletion [11].

Data from the plaque assay indicated that the titer of each virus, ranging from 1×10^{10}–4×10^{10} pfu/ml, was very similar. Since the plaque assay was determined in 293 cells, it is critical to know whether each virus has an infectivity similar to that of our target PC-3 cells. As shown in Figure 3B, the FACS results demonstrated that no C-CAM1 expression was detected in the AdCAM101-infected cells, because they expressed the antisense C-CAM1 mRNA. In contrast, the numbers of cells infected by each virus at 100 m.o.i. (Fig. 3A,C–F) reached a plateau. Therefore, we decided to use a lower dose of virus to test its tumor suppression function and in order to avoid any artifact due to viral toxicity.

Determination of Expression and Function of Mutated C-CAM1 Protein in PC-3 Cells by Various C-CAM1 Adenoviruses

Once these C-CAM1 mutant viruses were generated, we performed both Northern and Western blot analyses to examine the size of C-CAM1 transcript from infected PC-3 cells. PC-3 cells were infected with different clones of viruses at 10 m.o.i. As shown in Figure 4A, no detectable levels of C-CAM mRNA were found in control PC-3 cells. A full-length C-CAM1 mRNA was detected in PC-3 cells infected with either AdCAM101 or AdCAM902 viruses by a double-stranded cDNA probe. In contrast, a variable-sized C-CAM mRNA transcript was detected in PC-3 cells infected with the rest of the C-CAM1 mutant viruses. Western blot analysis (Fig. 4B) indicated that both AdCAM902 and AdCAMF488 expressed a C-CAM1 protein with 105 kDa. As expected, the molecular weight of mutated C-CAM1 protein induced by each mutant virus was smaller than that of wild-type C-CAM1 protein (Fig. 4B).

The cell adhesive assay was used as a functional test for these deletion mutants. Data in Figure 5 indicate that the control cells and PC-3 cells infected with AdCAM101 did not show any increase in intercellular adhesion. However, cells infected with either AdCAM902 or viruses containing the first Ig domain (such as AdCAMF488, AdCAMH458, and AdCAMG454) showed the same degree of cell adhesion function. In contrast, AdCAMΔD1, a mutant with a deletion of the first Ig domain, failed to elicit any intercellular adhesion in PC-3 cells, indicating that the first Ig domain is critical for the cell adhesive activity of the C-CAM1 molecule.

Change in Tumor Suppression Activity of C-CAM Mutants

To test the tumor suppression function of each C-CAM1 adenovirus, we infected PC-3 cells with the same titer of viruses overnight. Cells were trypsinized into single-cell suspensions: 1×10^4 cells were sub-

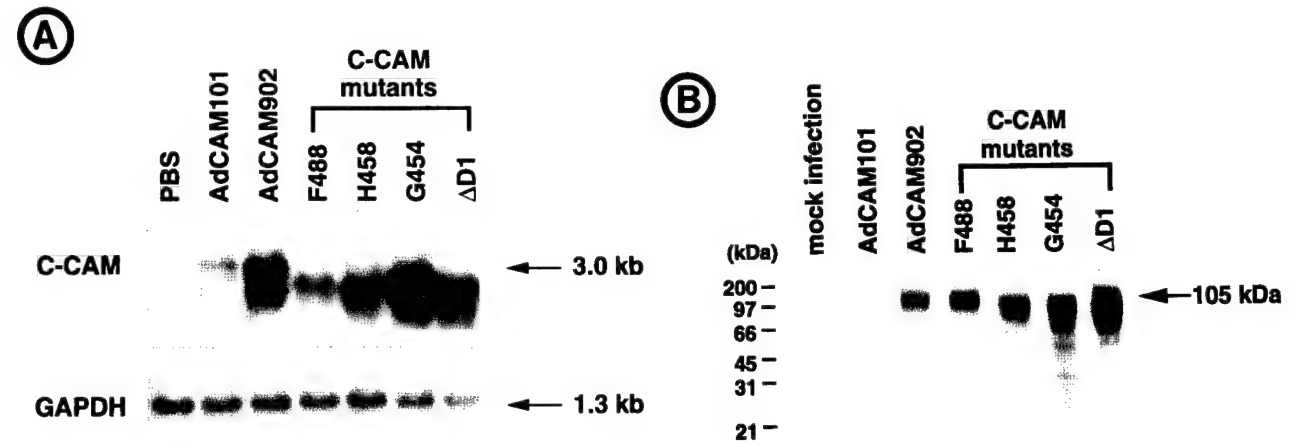

Fig. 4. Characterization of C-CAM1 expression in PC-3 cells by infecting the various C-CAM1 adenoviruses. C-CAM1 expression in PC-3 cells infected with the various C-CAM1 viruses was determined by both Northern and Western blot analyses. In Northern blot analysis (**A**), both a random primer radiolabeled C-CAM1 probe [8] and GAPDH as an internal control were used. In Western blot analysis (**B**), Ab669 [2] was used to detect the presence C-CAM1 protein.

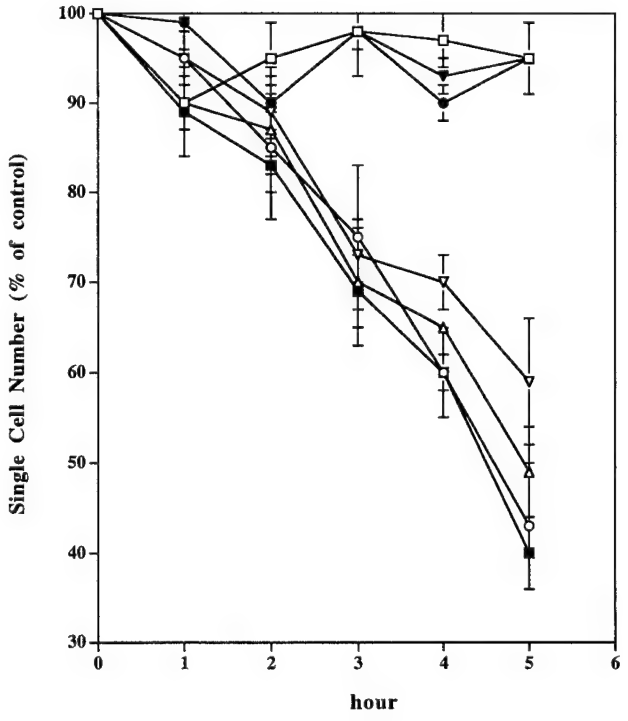

Fig. 5. Determination of cell adhesion activity from various C-CAM1 constructs. PC-3 cells were infected with each virus for 24 hr, and then the cells were trypsinized into a single-cell suspension. One million cells from each infection were incubated at room temperature with constant mixing. The percentage of single cells was determined at the times described previously [2] as indicative for the increment in cell adhesion activity. Mock infection (□), AdCAM902 (○), AdCAM101 (●), AdCAMF488 (△), AdCAMH458 (■), AdCAMG454 (▽), AdCAMΔD1 (▼).

jected to FACS analysis for determining the percentage of positive cells prior to injection, and 1×10^6 cells were injected into the flank of athymic nude mice. Tumors became palpable 5 weeks after injection; tumor incidence and volume were determined during week 8. In Table IA, data indicate that the tumor-suppression effect induced by C-CAM1 adenovirus was dose-dependent. However, at a low dose of virus (5 m.o.i.), we found that the tumor suppression effect was not very significant. At 50 m.o.i., data from both tumor incidence and volume clearly indicate that both the AdCAMF488 and AdCAMΔD1 still retained their tumor suppression function, as observed with AdCAM902. AdCAMΔD1 showed a decrease in its tumor suppression function, which may have been due to the low infectivity evidenced by FACS results (61% positive cells). In contrast, AdCAMH458 and AdCAMG454 decreased or lost their suppression function. AdCAM101, a control virus, showed no tumor suppression effect.

In the second experiment (Table IB), we reduced the viral titer (m.o.i. = 20) to avoid any overdose of viruses. We observed a similar tumor suppression effect from each C-CAM1 mutant virus at an m.o.i. of 20. Data from both experiments demonstrated that AdCAM902, AdCAMF488, and AdCAMΔD1 are potent tumor suppressors. However, the tumor suppression effect induced by AdCAMH458 was intermediate. In contrast, AdCAMG454 completely lost its tumor suppression function. Taken together, these data indicate that the intracellular domain, but not extracellular domain, of C-CAM1 is critical for its tumor suppression function.

TABLE I. Tumor Incidence and Tumor Volume of PC-3 Cells Inhibited by Either Wild-type C-CAM1 or C-CAM1 Deletion Mutant Adenoviruses

A. Treatment[a]	Percentage of positive cells[b]		Tumor incidence		Tumor volume (mm^3)[c]	
	m.o.i. = 5	m.o.i. = 50	m.o.i. = 5	m.o.i. = 50	m.o.i. = 5	m.o.i. = 50
Mock infection	0	0	10/12 (83%)		95 ± 27	
AdCAM101	0	0	6/6 (100%)	5/12 (42%)	105 ± 28	69 ± 19
AdCAM902	45	82	8/12 (66%)	0/12 (0%)	87 ± 32	0 ± 0
AdCAMF488	42	80	12/12 (100%)	1/12 (8%)	123 ± 33	153[d]
AdCAMH458	54	90	8/12 (66%)	7/12 (58%)	79 ± 28	34 ± 5
AdCAMG454	73	92	10/12 (83%)	8/12 (66%)	71 ± 14	67 ± 21
AdCAMΔD1	39	61	5/12 (42%)	6/12 (50%)	52 ± 20	21 ± 3

B. Treatment[a]	Percentage of positive cells,[b] m.o.i. = 20	Tumor incidence, m.o.i. = 20	Tumor volume (mm^3)[c] m.o.i. = 20
Mock infection	0	11/12 (92%)	62 ± 18
AdCAM101	0	12/12 (100%)	83 ± 30
AdCAM902	77	2/12 (17%)	8 ± 4
AdCAMF488	75	0/12 (0%)	0 ± 0
AdCAMH458	80	6/12 (50%)	34 ± 12
AdCAMG454	82	12/12 (100%)	65 ± 18
AdCAMΔD1	82	2/12 (17%)	7 ± 3

[a]Mock infection (PBS + 10% glycerol), AdCAM101 (antisense C-CAM1), AdCAM902 (sense C-CAM1 virus), AdCAMF488 (mutated C-CAM1 containing Tyr-488 → Phe-488), AdCAMH458 (C-CAM1 deletion mutant containing 458 amino acids), AdCAMG454 (C-CAM1 deletion mutant containing 454 amino acids), and AdCAMΔD1 (C-CAM1 mutant containing first Ig domain deletion).
[b]Percentage of positive cells were determined by FACS analyses.
[c]Tumor volume was calculated as described previously [3]; number represented mean ± SE.
[d]Only one tumor was observed; therefore, no standard error was calculated.

DISCUSSION

It is known that CAMs play a central role in coordinating tissue development and epithelial cell differentiation [12–14]. Moreover, altered CAM expression is often associated with carcinogenesis and the metastasis of many neoplasms [15–18]. For example, decreased expression of E-cadherin, a Ca^{2+}-dependent epithelial cell-specific CAM, is associated with the progression of several neoplasms [15,19–21]. Recent data from our laboratory and others demonstrated that C-CAM1, a Ca^{2+}-independent epithelial cell-specific CAM, can be a potent tumor suppressor in prostate cancer [3,4], colon carcinoma, and hepatocarcinoma [22–24]. Furthermore, a cytogenetic study also showed that deletion of the DCC gene, with a similar Ig-like structure as the C-CAM1, is found in colon cancer [25]. These data indicate that CAMs play a functional role in regulating the carcinogenic process.

C-CAM1 (also named cell-CAM105) is a 105-kDa cell-surface glycoprotein, first detected as the adhesion molecule mediating hepatocyte aggregation [26]. Previously, we observed that the C-CAM1 protein can be detected between cell boundaries of nonpolarized basal prostate epithelial cells in either prolonged castration prostate [1] or human fetal prostate [2]. These data imply that prostatic epithelial cells may use C-CAM1 as an intercellular adhesion molecule to achieve their cell-cell communication at this stage. This observation is supported by the expression of wild-type C-CAM1 protein in insect cells (i.e., Sf9 cells); using a baculoviral vector system resulted in cell aggregation of Sf9 cells [5]. Upon detailed dissection, of the function of four Ig domains of C-CAM1, Cheung et al. [5] showed that the first Ig domain is required for intercellular adhesion of the C-CAM1 molecule.

In addition to the extracellular domain of C-CAM1, the 71 amino acids of the intracellular domain are also required for the adhesion function of C-CAM1 [27]. Among these amino-acid sequences, there are two consensus sequences for both cAMP-dependent kinase and tyrosine kinase. Also, the putative tyrosine phosphorylation site localized in the antigen-receptor homology (ARH) motif is known to be essential for signal transduction in B-cells [28]. Our recent studies from both natural mutants of C-CAM (e.g., C-CAM3) [27] and deletion mutants generated by site-directed mutagenesis [10] further indicated that the potential Ser/Thr phosphorylation site (amino acids 455–458) in

the intracellular domain, in addition to the first Ig domain, was also critical for C-CAM's cell adhesion function.

Little is known about the functional domain(s) of C-CAM1 in modulating its tumor suppression activity in prostate cancer. Therefore, we decided to generate a variety of deletion mutants ranging from the deletion of the first Ig domain to the deletion of the "potential signal transduction motif" in the intracellular domain of the C-CAM1 molecule. As shown in Table I, both the first Ig domain and the tyrosine phosphorylation site (i.e., amino acid 488) did not play a significant role in modulating the suppression function of C-CAM1 in vivo. Interestingly, H458 lost half of the tumor suppression activity, suggesting that the C-terminal sequences (i.e., the 61 amino acids adjacent to amino acid 458), including ARH domain, may be critical for retaining the tumor suppression function of C-CAM1. Nevertheless, this study indicated that these four amino acids, containing a potential Ser/The phosphorylation site, are crucial for maintaining the tumor suppression function of C-CAM1 (Table I). Similar results were observed in breast cancer cells [29]. Taken together, two domains (amino acids 454–458 and 458–519) of C-CAM1 are crucial for its tumor suppression activity in human prostate cancer. Based on these results, we hypothesized that C-CAM1 protein phosphorylation modulated by protein kinase A may play an important role in suppressing prostate cancer growth. It is likely that the intracellular domain of C-CAM1 may also interact with other soluble factors to transduce its negative signal. An 80-kDa protein was recently identified as a potential interactive protein that is correlated with its growth inhibitory activity [30]. Furthermore, an interaction between C-CAM1 and structural protein may contribute to its biologic function. For example, three cytoplasmic proteins, α-, β-, and γ-catenin, are found to be associated with the cytoplasmic domain of E-cadherin [31]. These associated proteins, which are part of the adherent junction proteins, not only play important roles in maintaining cellular architecture [32], but also have been found to interact with other potential tumor suppressor gene products, e.g., APC [33,34]. Therefore, the potential interactive proteins associated with C-CAM1 warrant further investigation.

In this study, we observed that recombinant adenovirus appears to be an efficient vector to deliver exogenous DNA into target cells (Fig. 2 and Table I) in vitro. Also, our recent results showed that C-CAM1 adenovirus (i.e., AdCAM902) can effectively inhibit in vivo growth of tumors [4], indicating that the C-CAM1 adenovirus is a potent therapeutic agent in prostate cancer. However, because of its wide spectrum of host infectivity [35], recombinant adenovirus may express the transgene in nontarget cells, causing side effects in the host. To alleviate the undesired toxicity elicited by adenoviruses, in the prostate, tissue-specific promoters such as prostate-specific antigen [36] and the probasin gene [37] should be good candidates. Most importantly, this study demonstrated the critical functional domain of C-CAM1 in controlling the in vivo growth of human prostate cancer. Based on these results, C-CAM1 can be further engineered into a "pure" tumor suppressor by removing unnecessary residues, which may increase the therapeutic index for this molecule. Furthermore, identifying the signal pathway elicited by C-CAM1 in prostate cancer can provide a new strategy in fighting this disease.

ACKNOWLEDGMENTS

This work was supported in part by National Institutes of Health grant CA 59939 and an ARMY grant (to J.-T.H.). We thank Dr. John D. McConnell for his critical reading of the manuscript.

REFERENCES

1. Hsieh JT, Lin SH. Androgen regulation of cell adhesion molecule (CAM) gene expression in rat prostate during organ degeneration: C-CAM belongs to a new class of androgen-repressed genes associated with enriched stem/amplifying cell population after prolonged castration. J Biol Chem 1994;269: 3711–3716.
2. Kleinerman D, Troncoso P, Lin SH, Pisters LL, Sherwood ER, Brooks T, von Eschenbach AC, Hsieh JT. The expression of an epithelial cell adhesion molecule (C-CAM) in human prostate development and in prostate carcinoma: implication as a tumor suppressor. Cancer Res 1995;55:1215–1220.
3. Hsieh JT, Luo W, Song W, Wang Y, Kleinerman D, Van NT, Lin SH. Tumor suppressive role of an androgen-regulated epithelial cell adhesion molecule (C-CAM) in prostate carcinoma cell revealed by sense and antisense approaches. Cancer Res 1995;55: 190–197.
4. Kleinerman D, Zhang WW, von Eschenbach AC, Lin SH, Hsieh JT. Application of a tumor suppressor gene, C-CAM, in androgen-independent prostate cancer therapy: a preclinical study. Cancer Res 1995;55:2831–2836.
5. Cheung PH, Luo W, Qiu Y, Zhang X, Earley K, Millirons P, Lin SH. Structure and function of C-CAM1. J Biol Chem 1993;268: 24303–24310.
6. Zhang WW, Fang X, Branch CD, Mazur W, French BA, Roth JA. Generation and identification of recombinant adenovirus by liposome-mediated transfection and PCR analysis. Biotechniques 1993;15:868–872.
7. Zhang WW, Koch PE, Roth JA. Detection of wild-type contamination in a recombinant adenoviral preparation by PCR. Biotechniques 1995;18:444–447.
8. Culic O, Huang QH, Flanagan D, Hixson DC, Lin SH. Molecular cloning and expression of a new rat liver cell-CAM105 isoform. Biochem J 1992;285:47–53.
9. Lin SH, Culic O, Flanagan D, Hixson DC. Immunochemical characterization of two isoforms of rat liver ecto-ATPase that show an immunological and structural identity with a glyco-

protein cell-adhesion molecule with Mr 105,000. Biochem J 1991; 278:155–161.
10. Lin SH, Luo W, Earley K, Cheung P, Hixson DC. Structure and function of C-CAM1: effects of the cytoplasmic domain on cell aggregation. Biochem J 1995;311:239–245.
11. Jones N, Shenk T. An adenovirus type 5 early gene function regulates expression of other early viral gene. Proc Natl Acad Sci USA 1979;76:3665–3669.
12. Edelman GM. Cell adhesion and the molecular processes of morphogenesis. Annu Rev Biochem 1985;54:135–169.
13. Odin P, Asplund M, Busch C, Obrink B. Immunohistochemical localization of cell-CAM 105 in rat tissues: appearance in epithelia, platelets, and granulocytes. J Histochem Cytochem 1998;36: 729–739.
14. Takeichi M. The cadherins; cell-cell adhesion molecules controlling animal morphogenesis. Development 1988;102:639–655.
15. Edelman GM, Crossin KL. Cell adhesion molecules: Implication for a molecular histology. Annu Rev Biochem 1991;60:155–190.
16. Nicolson GL. Metastatic tumor cell interactions with endothelium, basement membrane and tissue. Curr Opin Cell Biol 1989; 1:1009–1019.
17. McCormick BA, Zetter B. Adhesive interactions in angiogenesis and metastasis. Pharmacol Ther 1992;53:239–260.
18. Chen W, Obrink B. Cell-cell contacts mediated by E-cadherin (uvomorulin) restrict invasive behavior of L-cells. J Cell Biol 1991;114:319–327.
19. Frixen UH, Behrens J, Sachs M, Eberle G, Voss B, Warda A, Lochner D, Birchmeier W. E-cadherin-mediated cell-cell adhesion prevents invasiveness of human carcinoma cells. J Cell Biol 1991;113:173–185.
20. Bussemakers MJ, van Moorselaar RJ, Giroldi LA, Ichikawa T, Isaacs JT, Takeichi M, Debruyne FM, Schalken JA. Decreased expression of E-cadherin in the progression of rat prostate cancer. Cancer Res 1992;52:2916–2922.
21. Umbas R, Schalken JA, Aalders TW, Carter BS, Karthaus HF, Schaafsma HE, Debruyne FM, Isaacs WB. Expression of the cellular adhesion molecule E-cadherin is reduced or absent in high-grade prostate cancer. Cancer Res 1992;52:5104–5109.
22. Hixson DC, McEntire KD. Detection of an altered form of cell-CAM105 on rat transplantable and primary hepatocellular carcinomas. Cancer Res 1989;49:6788–6794.
23. Rosenberg M, Nédellec P, Jothy SS, Fleiszer D, Turbide C, Beauchemin N. The expression of mouse biliary glycoprotein, a carcinoembryonic antigen-related gene, is down-regulated in malignant mouse tissues. Cancer Res 1993;53:4938–4945.
24. Neumaier M, Paululat S, Chan A, Matthales P, Wagnerer C. Biliary glycoprotein, a potential human cell adhesion molecule, is down-regulated in colorectal carcinoma. Proc Natl Acad Sci USA 1993;90:10744–10748.
25. Fearon ER, Cho KR, Nigro JM, Kern SE, Simons JW, Ruppert JM, Hamilton SR, Preisinger AC, Thomas G, Kinzler KW, Vogelstein B. Identification of a chromosome 18q gene that is altered in colorectal cancers. Science 1990;247:49–56.
26. Ocklind C, Obrink B. Intercellular adhesion of rat hepatocytes. Identification of a cell surface glycoprotein involved in the initial adhesion process. J Biol Chem 1982;257:6788–6795.
27. Cheung PH, Culic O, Qiu Y, Earley K, Thompson NL, Hixson D, Lin SH. The cytoplasmic domain of C-CAM is required for C-CAM-mediated adhesion function: studies of a C-CAM transcript containing an unspliced intron. Biochem J 1993,295:427–435.
28. Cambier JC, Campbell KS. Membrane immunoglobulin and its accomplices: new lessons from an old receptor. FASEB J 1992; 6:3207–3217.
29. Luo W, Wood CG, Early K, Hung M, Lin SH. Suppression of tumorigenicity of breast cancer cells by an epithelial cell adhesion molecule (C-CAM1): the adhesion and growth suppression are mediated by different domains. Oncogene 1997;14:1697–1704.
30. Luo W, Early K, Tantingco V, Hixson DC, Liang TC, Lin SH. Association of an 80 kDa protein with C-CAM1 cytoplasmic domain correlates with C-CAM1-mediated growth inhibition. Oncogene 1998;16:1141–1147.
31. Takeichi M. Cadherin cell adhesion receptors as a morphogenetic regulator. Science 1991;251:1451–1455.
32. Geiger B. Membrane-cytoskeleton interaction. Biochim Biophys Acta 1983;737:305–341.
33. Rubinfeld B, Souza B, Albert I, Muller O, Chamberlain SSH, Masiarz FR, Munemitsu SS, Polakis P. Association of the APC gene product with β-catenin. Science 1993;262:1731–1734.
34. Su LK, Vogelstein B, Kinzler KW. Association of the APC tumor suppressor protein with catenins. Science 1993;262:1734–1737.
35. Grunhaus A, Horwitz MS. Adenovirus as cloning vector. Semin Virol 1992;3:237–252.
36. Pang S, Taneja S, Dardashti K, Cohan P, Kaboo R, Sokoloff M, Tso CL, Dekernion JB, Belldegrun AS. Prostate tissue specificity of the prostate-specific antigen promoter isolated from a patient with prostate cancer. Hum Gene Ther 1995;6:1417–1426.
37. Greenberg NM, DeMayo FJ, Sheppard PC, Barrios R, Lebovitz R, Finegold M, Angelopoulou R, Dodd JG, Duckworth ML, Rosen JM, Matusik RJ. The rat probasin gene promoter directs hormonally regulated expression of a heterologous gene specifically to the prostate in transgenic mice. Mol Endocrinol 1994;8: 230–239.

A Novel GTPase Activating Protein that Interacts with DOC-2/DAB2: A downstream effector leading to the suppression of mitogenic signal transduction in prostate cancer

Zhi Wang[†], Ching-Ping Tseng[‡], Rey-Chen Pong[†], Hong Chen[†], John D. McConnell[†], Nora Navone[§] and Jer-Tsong Hsieh[†]*

[†]Department of Urology, University of Texas Southwestern Medical Center at Dallas Dallas, TX 75390-9110 and [§]Department of GU Medical Oncology, University of Texas M.D. Anderson Cancer Center, Houston, TX 77030

[‡] Current address: School of Medical Technology, Chang Gung University, Tao-Yuan, Taiwan

* To whom correspondence should be addressed:
J.T. Hsieh, Ph.D.
University of Texas Southwestern Medical Center
Department of Urology
5323 Harry Hines Blvd.
Dallas, TX 75390-9110
(phone) 214-648-3988
(fax) 214-648-8786
(email) JT.Hsieh@UTSouthwestern.edu

Running Title: DIP1/2, a novel DOC-2/DAB2 interactive protein.

Summary

We describe the cloning of DIP1/2, a novel gene that interacts with the N-terminal DOC-2/DAB2. DOC-2/DAB2 is a member of the disable gene family. Its down regulation is associated with several neoplasms, and serine phosphorylation of its N-terminal modulates DOC-2/DAB2's inhibitory effect on AP-1 transcriptional activity. DIP1/2 is a novel GTPase-activating protein containing a Ras GAP homology domain (N-terminus) and two other unique domains (i.e., 10 proline repeats and leucine zipper). Interaction between DOC-2/DAB2 and DIP1/2 is detected in normal tissues such as the brain and prostate. Altered expression of these two proteins is often detected in prostate cancer cells. Indeed, presence of DIP1/2 effectively blocks mitogen-induced gene expression and inhibits the growth of prostate cancer. Thus, DOC-2/DAB2 and DIP1/2 appear to represent a unique negative regulatory network that maintains cell homeostasis.

Introduction

DOC-2/DAB2 (differentially expressed in ovarian carcinoma 2 / *disabled*-2) is identified in normal human ovarian epithelial cells but absent in ovarian cancer cell lines (1, 2). Absence of DOC-2/DAB2 expression is associated with malignant cells including mammary, prostate, and ovary (2, 3, 4). Increased expression of DOC-2/DAB2 inhibits the growth of several cancer cells (4, 5), which suggests that it functions as a tumor suppressor. DOC-2/DAB2 also appears to be a phosphoprotein, and its phosphorylation can be regulated by several stimuli (4, 6). We recently demonstrated that DOC-2/DAB2 expression is significantly increased in the enriched basal cell population with stem cell potential of the degenerated rat prostate (4), suggesting that DOC-2/DAB2 may play an important role in regulating the homeostasis of epithelial differentiation. Amino acid sequence analysis predicts that DOC-2/DAB2 is a potential signaling molecule. Its N-terminus shares 54% homology with mouse DAB1 protein that can be phosphorylated by Src, and the disruption of the *DAB1* gene can cause developmental defects in central neurons (7, 8). In addition, we and other also show that C-terminal DOC-2/DAB2 containing proline-rich domains can bind to Grb2 proteins (9, 10). Thus it appears that DOC-2/DAB2 is involved in modulating Ras signaling pathway.

To understand biochemical function of DOC-2/DAB2, we identified a key amino acid residue (S^{24}) in its N-terminus. The phosphorylation of this residue by protein kinase C (PKC) activator-12-*O*-tetradecanoylphorbol-13-acetate (TPA), can modulate its inhibitory activity on TPA-induced gene transcription (10). These data indicate that the DOC-2/DAB2 protein, particularly its N-terminus, is a potent negative regulator for PKC-elicited signal pathway. However, little is known about the down stream effector(s) mediated by DOC-2/DAB2.

In this study, we employed a yeast two-hybrid system to identify DIP1/2 as an immediate DOC-2/DAB2 interactive protein. DIP1/2, a novel Ras GTPase-activating protein (GAP), interacts with the N-terminal of DOC-2/DAB2. We cloned DIP1/2, characterized it as an immediate downstream effector of DOC-2/DAB2, and delineated its functional role in mitogen-induced gene expression and growth inhibition of prostate cancer.

Experimental Procedures

Cell Cultures

Three human prostate cancer cell lines (TSU-Pr1, LNCaP, C4-2) and COS cells were maintained in T medium supplemented with 5% fetal bovine serum (4). PrEC, a primary prostatic epithelial cell derived from a 17-year-old juvenile prostate, was maintained in a chemical-defined medium purchased from Clonetics. PZ-HPV-7, a cell line derived from the peripheral zone of a normal prostate (11), was maintained in T medium containing 5% fetal bovine serum. $MDAPCa_{2a}$ and $MDAPCa_{2b}$ cell lines were derived from patients with bony metastasis (12). Three additional primary prostatic epithelial cells, derived from either cancer lesions (SWPC1, SWPC2) or adjacent normal tissue (SWNPC2), were obtained from patients with prostate cancer who had had radical prostatectomy. All these cells were maintained in the same medium as PrEC. Corresponding antibody staining indicated that all primary cells were cytokeratin positive and vimentin negative.

Yeast Two-hybrid Screening

Using primers 5'-GAATTCCCCGTCATGTCTAACGAA-3' and 5'-GGATCCTAACTGAGGCTTTGGTCGAGG-3', and DOC-2/DAB2 cDNA as a template, we generated an 823 bp fragment corresponding to the 5' end of the cDNA.

The polymerase chain reaction (PCR)-amplified fragment was sequenced before it was subcloned in-frame into pVJL11 vector as a bait construct. Equal amounts of constructed bait vector and pVP16 rat brain cDNA library vector were co-transformed into the yeast strain of L40, and the transformed yeast were plated on SD-L-T-H (synthetic medium lacking amino acids of leucine, tryptophan, and histidine) plates with 5 mM 3-AT (3-amino-trizol). Only those colonies that had β-galactosidase activities were further analyzed. Plasimds from those positive clones were rescued and transformed into *E.coli* HB101 strain for further amplification.

Four rounds of phage library screening were performed with a rat brain λ ZAP phage library (Stratagene) to clone the full-length cDNA of DIP1/2. After DNA sequencing for each positive clone, the full-length cDNA of DIP1/2 was assembled with the appropriate restriction enzyme digestion.

Northern Blot

Total RNA from various organs of the male rat was isolated with RNAzol (TEL-TEST). Twenty micrograms of total RNA per lane were separated on 1% formaldehyde agarose gel, transformed onto Zeta-Probe membrane (Bio-RAD), then hybridized with ^{32}P-labeled DIP1/2 or GAPDH cDNA probe.

Generation of the anti-DIP1/2 Polyclonal Antibody

A peptide sequence (CTNPTKLQITENGEFRNSSNC) corresponding to DIP1/2 amino acid residues 976 to 996—with an extra cysteine at the N-terminus as a linker—was synthesized and used as the antigen to immunize rabbits for generating polyclonal antibody by Zymed Laboratory. After 7 weeks, rabbits were sacrificed to collect antiserum after the fourth boosting injection of antigen. SulfoLink gel (Pierce) was coupled with the synthetic peptide, then blocked with 50 mM cysteine in 50 mM Tris, 5 mM EDTA, and pH 8.5 was then washed with 1M NaCl. Antibodies against DIP1/2 were first purified by slowly passing the antiserum to the coupled SulfoLink gel. After washing with 5 column's volume of 1 M NaCl, they were eluted with elution buffer from Sulfolink Kit (Pierce). Purified antibodies were dialyzed overnight against 4 L of deionized water at 4 °C.

Coimmunoprecipitation and Immunobloting

COS cells were co-transfected with a series of T7-tagged deletion mutants, wild types of DOC-2/DAB2 vectors, and HA-tagged DIP1/2 vector. Cells were lysed with a lysis buffer (50mM Tris, pH 7.5, 1% NP-40, 1 mM EDTA) and a cocktail of protease and phosphotase inhibitors (1 mM phenylmethylsulfonylfluoride, 0.2 mM sodium orthovanadate, 0.1 mM sodium fluoride, 10 µg/ml aprotinin, 10 µg/ml leupeptin). The supernatant was collected and incubated overnight with either 60 µl of T7-antibody conjugated-agarose beads solution (50% actual volume) or 60 µl of protein A agarose

bead with 10 μg HA-antibody at 4 °C. After incubation, pellets were washed 8 times and subjected to a 10% SDS-PAGE and Western blot analysis.

Purification of the GST Fusion Protein and Ras GAP Activity Assays

The minimal GAP domain of DIP1/2 cDNA was amplified by PCR using primers 5'-GGGATCCCAGAACGCAACAGC-3' and 5'-AGAATTCTTAGCTTGAGCTGCGG GCAGG-3'. The amplified fragment was subcloned in-frame into the pGEX-5X vector and transformed into the *E.coli* strain of BL21. The bacteria culture was induced with 2.5 mM IPTG at 37 °C for 4 hours. The bacterial pellet was washed once with cold PBS. After spin, the pellet was re-suspended in PBS and subjected, five times, to 30-second sonication. The GST-GAP fusion protein was purified according to the manufacture's manual (Roche), and the purified protein was analyzed using 10% SDS-PAGE analysis and followed by GELCODE Blue staining (Pierce).

Assay of Ras GAP activity *in vitro* was performed according to Kim *et al* (13). To prepare GTP-bound Ras protein, 0.25 μM human recombinant Ras protein (Cal Biochem) was incubated with 20 nM [γ-^{32}P]GTP (6,000Ci/mmol, DuPont-NEN) in a buffer containing 20 mM HEPE (pH 7.3), 1 mM EDTA, 2 mM DTT, and 1 mg/ml BSA for 5 minutes at room temperature. Up to 1 μg of either GST-GAP or GST protein alone was added into a buffer containing 20 mM HEPE, pH7.3, 5 mM $MgCl_2$, and 1 mM DTT. The loaded Ras was then incubated with either GST-DIP1/2 or GST for the indicated

time, and the reaction was stopped by adding 5 volumes of ice-cold 20 mM HEPE, pH 7.3, and 1 mM $MgCl_2$. The reaction mixture was then filtered through 0.45 μm HA membrane (Millipore). Filters were air-dried then subjected to scintillation count.

C4-2 cells were transfected with either HA-tagged Ras alone or HA-tagged Ras and DIP1/2. Two days after transfection, cells were treated overnight with T medium without serum, and 100 ng/ml EGF was added for 20 minutes. Then, cells were lysed with lysis buffer (PBS with 5mM $MgCl_2$ and 1% Triton X-100). The whole lysate was spun down, and the supernatants were added with 10 μl of Raf-conjugated agarose beads (Upstate Biochetech). The mixtures were incubated at 4 °C for 30 minutes. Pellets were spun down and washed 4 times with the same lysis buffer, and 20 ml 1x SDS-PAGE sample buffer was added to the pellets and incubated at 100 °C for 3 minutes. Treated samples were loaded on SDS PAGE gel, and Ras-Raf binding was detected using Western blot.

Generation of pCI-DIP1/2 mutants and pGEX-5X-DIP1/2 constructs

To make mutants of DIP1/2 and the GST fusion DIP, the QuikChange™ Site-Directed Mutagenesis Kit was employed. Site-directed mutagenesis was performed by PCR according to the manufacture (Stratagen). Oligonucleotide used for each mutant was 5'-GGACAATGAGCACCTCATCTTTCTGGAGAACACATTGGCCACCAAGG-3'. Briefly described, after denatuing the wild type plasmids the oliginucleotide primer

was annealed with template DNA then extend with PfuTurbo DNA polymerase. After PCR, the methylated and non-mutated parental DNA template was digested with DpnI. The XL-1 Blue cells were then transformed with DpnI-treated DNA for selecting the mutated DNA. Mutants were verified by sequencing.

In vitro Characterization of the Effect of DIP1/2 on Prostate Cancer

To determine the effect of DIP1/2 on prostate cancer cells, we studied: 1) gene transcription using either SRE or TRE reporter gene assays, and 2) cell growth using both crystal violet and colony formation assays.

For reporter gene assay, C4-2 cells were transiently transfected with either SRE or TRE reporter plasmids in the combination of DIP1/2, ΔB, and ΔB-S^{24}A expression vectors. Two days after transfection, T medium with 0.5 % FBS was changed for another 24 hours, then either 50 ng/ml of EGF or 100 ng/ml TPA was added to the cells for an additional 14 hours. Luciferase activity assays were performed as described previously (10).

Using lipofectamine (Life Technology), C4-2 cells (2×10^5) were transfected with 2 μg of pCI-DIP1/2 or 2 μg of pCI-neo (control). Two days after transfection, cells were selected with G418 (800 μg/ml), and an individual colony was cloned by ring isolation (4). The *in vitro* growth rate of each clone was determined by plating cells in a 24-well plate at a density of 5,000 cells/well with T medium containing 2% TCM and 0.5% FBS.

At the indicated days, cell numbers were determined by crystal violet assay (14, 15).

Colony formation assay was carried out according to Yeung *et al* (16).

Results

Identifying and Cloning DIP cDNA

DOC-2/DAB2's first 260 amino acids were used as a "bait" sequence in the yeast two-hybrid system to search for protein(s) that interacts with the N-terminal DOC-2/DAB2 (17). Of 10,000 transformants screened, 36 positive clones were selected, and two positive clones (DIP1, DIP2) were further analyzed. These two clones shared overlapping sequence and were identical. However, as neither alone contained a full-length sequence, we designated the full-length sequence "DIP1/2."

To obtain the full-length cDNA of DIP1/2, a λ ZAP cDNA library from a rat brain was screened. Eleven clones spanned about 6.3 kb and represented two different sizes of DIP1/2 mRNA transcripts with different 5' untranslated sequences (Figure 1A). The full-length DIP1/2 cDNA has been deposited into GenBank (AF236130). The DIP1/2 was predicted to have an open reading frame of 996 amino acids and a calculated molecular mass of 110 kD.

According to the deduced protein sequence, DIP1/2 appears to be a novel protein with several potential functional domains (Figure 1B). Its key feature is the RasGAP homology domain, which spans from residues 177 to 409 and is present in all members of the RasGAP family (18). Also, DIP1/2 had a stretch of 10 proline

repeats (residues 727 to 736) with the capacity to bind to proteins containing an SH3 domain (19) and a leucine zipper dimerization domain (residues 842 to 861) for protein dimerization (20). The amino acid sequence alignment of DIP1/2's GAP domain with other RasGAP proteins (Figure 1C)—including p120GAP, *Homo sapiens* neurofibromine (hNF1), *Rattus norvegicus* RasGAP (rnGAP), nGAP, and Synaptic RasGAP (SynGAP)—shows that DIP1/2 contains all the critical consensus amino acids for RasGAP activity (21). This suggests that DIP1/2 can function as a RasGAP.

Characterizing the DIP1/2 Expression Profile

Northern blot analysis indicated that steady-state levels of DIP1/2 mRNA are detected in brain, lung, kidney, thymus, bladder, and skeletal muscle tissue (Figure 2A). At least two sizes of RNA transcripts (9.6 kb, 6.9 kb) were found in brain tissue that may correspond to these two individual cDNAs identified from the brain cDNA library. Steady-state levels of DIP1/2 mRNA were not detected in several urogenital organs including the ventral prostate, dorsal lateral prostate, seminal vesicle, and coagulating gland. However, increased levels of DIP1/2 mRNA (Figure 2A) were detected in NbE (Noble rat prostate epithelia) and VPE (Sprague-Dawley rat prostate epithelia) from basal cells of the ventral prostate. Increased levels were not detected in stromal cells (i.e., NbF and VPF) from the same animals. This indicates that DIP1/2 preferentially expresses in the prostatic basal epithelial cells. Further Northern

analysis (Figure 2B) indicated that expression of DIP1/2 mRNA increased in degenerated prostates in a time-dependent manner, and the expression patterns of DIP1/2 and DOC-2/DAB2 mRNA concur. These findings suggest that both genes co-express in the enriched basal cell population during prostate degeneration (Figure 2B).

A polyclonal antibody was raised against a synthetic peptide derived from the C-terminal DIP1/2. With this antibody, a single protein band with a molecular mass of 110 kDa was detected from the *in vitro* transcription and translation of DIP1/2 cDNA (Figure 3A). Because at least two DIP1/2 mRNA transcripts were detected in brain tissue, we examined the expression profile of DIP1/2 protein in brain tissue. As expected, there were two sizes of DIP1/2 protein in the rat brain (molecular masses of 110 kDa and 135 kDa, respectively) (Figure 3A). To further test the specificity of this antibody, serum was incubated with increasing concentrations of synthetic peptide of DIP1/2, ranging from 20 μg/ml to 200 μg/ml, prior to probing with the blotted membrane. Results (Figure 3B) indicated that the synthetic peptide effectively competes with the antibody in ability to bind to the DIP1/2 protein.

We also examined the protein expression profile of DIP1/2 in different rat organs (Figure 3C). Results indicated that DIP1/2 expression is not as abundant as that of DOC-2/DAB2. We could only detect DIP1/2 in lung, bladder, and thymus tissue was consistent with the Northern analysis (Figure 2A). However, expression of

DOC-2/DAB2 appeared ubiquitous in all tissues examined. Consistent with elevated DIP1/2 mRNA levels detected in degenerated prostate (Figure 2B), increased protein expression of DIP1/2 was seen in degenerated prostate tissue (Figure 3D). As they were parallel with DOC-2/DAB2 levels, these results (Figure 3D) suggest a pairwise control of both DIP1/2 and DOC-2/DAB2 proteins.

To further understand the profile of DIP1/2 and DOC-2/DAB2 expression in prostate cancer, we screened a variety of prostate cancer cells. Figure 3E shows that the antibody also recognizes the homologue of human DIP1/2 (hDIP1/2), and the molecular weight of hDIP1/2 is the same as rat DIP1/2. This implies that the sequence of DIP1/2 may be conserved among species. We also found that DIP1/2 and DOC-2/DAB2 proteins were present in both normal primary epithelial cells (PZ-HPV-7, PrEC, and SWNPC2) and primary tumors (SWPC1 and SWPC2). However, a significant decreased expression of DIP1/2 was detected in several metastatic cell lines such as TSU-Pr1, LNCaP, C4-2, $MDAPCa_{2a}$, and $MDAPCa_{2b}$, cancer cell lines. We believe this indicates that DIP1/2 is involved in the progression of prostate cancer.

Specific Interaction Between DIP1/2 and DOC-2/DAB2

Because data from the yeast two-hybrid screening indicated that DIP1/2 and DOC-2/DAB2 directly interact, we further examined whether these proteins also

physically interact in mammalian cells. Cells were co-transfected with T7-tagged, wild type DOC-2/DAB2 (p59 and p82) or DOC-2/DAB2 deletion mutants (ΔN, N-terminal deletion mutant, and ΔB, C-terminal deletion mutant) (10), and a HA-tagged DIP1/2 construct. Figure 4A shows that when cell lysates were immunoprecipitated with T7-antibody conjugated agarose beads and then probed with HA-antibody, DIP1/2 can be co-immunoprecipitated with p59, p82, and ΔB. In contrast, ΔN failed to pull down DIP1/2. But, using HA-antibody for immunoprecipitation and then probing with T7-antibody, we demonstrated that DIP1/2 protein could interact with the wild type DOC-2/DAB2 protein and the ΔB protein, but not with the ΔN protein (Figure 4B). Taken together, these data indicate that DIP1/2 protein only interacts with N-terminal, but not C-terminal, DOC-2/DAB2 protein. Furthermore, Figure 4C shows that levels of protein expression in each transfection were identical, which rules out any experimental artifact.

We further examined whether these two native proteins interact with each other using brain and prostate as tissue sources. Using antibodies against either DOC-2/DAB2 or DIP1/2 in a co-immunoprecipitation experiment, we demonstrated that endogenous DIP1/2 and DOC-2/DAB2 proteins were present in the same immuno complex (Figure 4D). Since DAB1 and DOC-2/DAB2 share a high degree homology at the PTB domain, we also examined whether mouse DAB1 can interact with DIP1/2.

Two mouse DAB1 cDNA clones (PTB, B3) were used (22), and we found that DIP1/2 interacts with DAB-PTB (aa 29-197) but not DAB-B3 (aa107-243). Because DAB-B3 contains partial PTB sequences.

Function of DIP1/2 *in vitro* and *in vivo*

Due to the high sequence homology between DIP1/2 and other RasGAPs, we thought it likely that DIP1/2 facilitates RasGTPase activity. To test this, we prepared a GST-DIP1/2 fusion protein containing the minimal RasGAP domain (23), and either this fusion protein or GST protein was incubated with human recombinant [γ-^{32}P] GTP-bound Ras protein. The increasing amounts of GST-DIP1/2 (ranging from 0.2 to 1 μg) stimulated Ras GTPase activity in a dose-dependant manner (Figure 5A). Conversely, control GST protein (1 μg) had no effect on RasGTPase activity.

To further test the RasGAP activity of DIP1/2, we created a DIP1/2 cDNA construct (DIP1/2$_m$) as a control that had a point mutation (R220L) which disrupts GAP activity. As sown in Figure 5B, the GST-DIP1/2 mutant did not have any GAP activity towards Ras. These data clearly demonstrate that DIP1/2 can stimulate RasGTPase activity *in vitro.*

Early study of Ras signal transduction indicates that Raf is an immediate downstream effector for Ras signaling (24). Because Raf binds tightly to the GTP-

bound form of Ras but not to the GDP-bound form, such differential affinity can be used to determine the GTP-bound status of Ras. To analyze the GAP activity of DIP1/2 *in vivo*, C4-2 cells (25) were transfected with vectors expressing either HA-tagged Ras, DIP1/2, or DIP1/2_m. After activating Ras using EGF, the GTP-bound form of Ras was precipitated with GST-RBD (GST-Raf containing Ras binding domain). Precipitated Ras was detected using the HA-antibody. Figure 5C shows, that in the presence of EGF, the amount of GTP-bound Ras increased over that of the control. Levels of the GTP-bound Ras significantly decreased in cells expressing DIP1/2, however, DIP1/2_m failed to stimulate RasGTPase in cells treated EGF. The whole cell lysates were examined for expression of DIP1/2 and Ras proteins, and results demonstrated that expressions of DIP1/2 and Ras were identical between each transfection. These results indicate that DIP1/2 can function as a RasGTPase activating protein *in vivo*. Therefore, we conclude that DIP1/2 functions as a Ras GAP *in vivo* and *in vitro*.

Regulation of the Ras-Raf Signaling Pathway by DIP1/2

Ras protein functions as an essential component in many intracellular signaling pathways responsible for differentiation, proliferation, and apoptosis (26). The Raf-MEK-ERK pathway is a key signal transduction pathway modulated by Ras protein (27). The downstream components of this pathway—including AP-1, which binds to

TRE (TPA response element), and EIK-1, which binds to SRE (serum response element)—subsequently activates gene expression (28-30). Since PKC is able to activate Raf/MEK/ERK axis (31, 32), we investigated the impact of DIP1/2 on this cascade. As shown in Figure 6A, in the absence of EGF, increased expression of DIP1/2 could inhibit the basal levels of SRE reporter gene activity in prostate cancer cells.

The presence of EGF increased the reporter gene activity at least 5-fold. However, DIP1/2 could inhibit the reporter gene activity in a dose-dependent manner. Using the same reporter gene assay, we found that DIP1/2 or ΔB alone can suppress SRE activity (Figure 6B), but co-expression of ΔB and DIP1/2 had an additive effect on the inhibition of SRE activity in the presence of TPA. These data indicate that physical interaction between DIP1/2 and DOC-2/DAB2 has functional impact on Ras-mediated signal transduction.

Previously we demonstrate that PKC-elicited DOC-2/DAB2 phosphorylation can block TPA-induced gene activity (10). Therefore, we investigated whether DIP1/2 is a mediator involved in this action. We employed C4-2 cell line because both DOC-2/DAB2 and DIP1/2 are not detectable. Either ΔB or DIP1/2 alone was able to inhibit TPA-induced TRE reporter gene activity (Table 1). Conversely, combing ΔB-S24A mutant with DIP1/2 failed to have any inhibitory effect because

S^{24A} in DOC-2/DAB2 is the key amino acid to modulate this activity. We observed an additive effect on inhibiting TRE reporter gene activity in the presence of ΔB and DIP1/2. In contrast, ΔB-S24A and DIP1/2 did not have any additive effect. Thus, the binding of DIP1/2 to ΔB can be enhanced by TPA, whereas ΔB-S24A can not (Figure 6C).

Biological Effect of DIP1/2 on Prostate Cancer Cells

Because DIP1/2 appears to be a negative regulator for the Ras-mediated pathway, it may function as a growth inhibitor. To test this, C4-2 cells (a tumorgenic human prostate cancer cell line) were transfected with a DIP1/2 expression vector. Initially, we observed that there were fewer surviving clones in the DIP1/2-transfected plate than in plasmid control-transfected cells despite the same number of cells being used in transfection (data not shown). After isolating two colonies (D1, D2)—confirmed by Southern blot (Figure 7A)—protein levels of DIP1/2 in the D2 subline were higher than those in the D1 subline (Figure 7B). Data from Figure 7C indicated that expression of DIP1/2 significantly inhibited the *in vitro* cell growth compared to the plasmid control. This inhibitory effect of both D1 and D2 correlated with their DIP1/2 protein levels (Figure 7B).

To rule out possible artifact from stable transfection, we examined the growth suppression of DIP1/2 in C4-2 cells using transient transfection (16). As shown in

Figure 8A, an elevated DIP1/2 expression—evidenced by Western blot (Figure 8B)—inhibited colony formation of C4-2 in a time-dependent manner. Conversely, increased DIP1/2_m expression did not effect colony formation of C4-2. These data indicate that DIP1/2's GAP activity modulates its growth inhibitory effect. DIP1/2 appears to be a potent growth inhibitor for prostate cancer.

Discussion

The DIP1/2 expression profile in tissue appears to be diverse. Both Northern and Western analyses (Figures 2A and 3C) indicate a high level of DIP1/2 mRNA expression in brain, thymus, and bladder tissue, and a low level in skeleton muscles, kidney, and liver tissue. But, no expression can be detected in several urogenital organs, including the ventral prostate, dorsolateral prostate, seminal vesicle, and coagulating gland. This unique pattern of tissue distribution implies that DIP1/2 may have a specific physiological function in each organ. For example, DIP1/2 expression is detected in the enriched basal cell population of degenerated prostate and in prostatic epithelial cell lines (such as NbE and VPE) derived from the basal cell population (Figure 2A), suggesting that DIP1/2 may be involved in prostate regeneration. This hypothesis can be supported by our results: (1) decrease or absence of either DIP1/2 or DOC-2/DAB2 is often detected in several metastatic human prostate cancer cell lines (Figure 3E); and (2) DIP1/2 appears to be a potent growth inhibitor for human prostate cancer cells (Figures 7 and 8). Ii is known that increased Ras activity is associated with high-grade metastatic prostate cancer, however, *RAS* mutation is rarely detected (33, 34). Our results suggest an underlying mechanism with which to account for this phenomenon. In addition to DIP1/2, we found that altered expression of p120GAP is associated with prostate cancer cells (data not

shown). Thus, our results indicate that altered RasGAP expression plays a critical role in the progression of prostate cancer.

The phosphorylation of S^{24} in DOC-2/DAB2, which is involved in inhibiting TPA-induced AP-1 activity (10), provides evidence for underlying functional mechanism of DOC-2/DAB2. In this study, our data indicate that DIP1/2 is an immediate downstream effector for DOC-2/DAB2 in both prostate and brain tissues (Figure 4) and the binding of DIP1/2 to DOC-2/DAB2 can be enhanced when the S^{24} residue in DOC-2/DAB2 is phosphorylated (Figure 6C). The most conserved region in DIP1/2 protein is the GAP domain, which has a high amino acid sequence homology (40 to 90%) compared to the GAP domains of other RasGAPs, and DIP1/2's GAP domain contains all 31 consensus amino acids of other RasGAPs. These consensus amino acid residues in the Ras GAP domain modulate RasGTPase activity (13). For example, R^{789} of p120GAP participates in catalysis and simultaneously stabilizes Q^{61} of Ras for optimal GTP-hydrolysis (35). Our data (Figures 5A and 5C) indicate that DIP1/2 has RasGAP activity *in vitro* and *in vivo*. Since R^{220} of DIP1/2 is equivalent to R^{789} of p120GAP, once R^{220} was altered (R220L), the single amino acid mutant of DIP 1/2 lost its RasGAP activity *in vitro* and *in vivo* (Figures 5B and 5C).

We demonstrate that co-expression of DIP1/2 and the N-terminal DOC-2/DAB2 (i.e., ΔB) has an additive effect on suppressing TPA-induced either SRE or TRE reporter gene activity (Figure 6B and Table 1). Therefore, we believe that the *in vivo* interaction of DIP1/2 with the N-terminal DOC-2/DAB2 plays a feed back mechanism to modulate PKC-induced gene activation. It is known that the modulation of Raf/MEK/ERK axis is also controlled by growth factors through their protein receptor tyrosine kinase. Our data indicate that DIP1/2 alone is also able to inhibit EGF-induced SRE reporter gene activity (Figure 6A). Therefore, this protein complex containing both DOC-2/DAB2 and DIP1/2 represents unique negative regulatory machinery to balance signals elicited by growth factors (such as EGF) or PKC activators (such as TPA).

In addition to the N-terminal RasGAP homology domain of DIP1/2, the proline-rich repeats and leucine zipper domains from its C-terminus may contribute to DIP1/2 activity. We found that the proline-rich repeats (residues 727 to 736) in DIP1/2 can interact with Grb2 (data not shown). Because Grb2 binds to SOS, a guanine nucleotide exchange factor critical for downstream signaling, the binding of DIP1/2 to Grb2 may interrupt Ras activation. It is also possible that DIP1/2 can interact with other proteins containing SH3 domain. On the other hand, leucine zipper domain (residues 842 to 861) of DIP1/2 may form a homodimer or a heterodimer with

other proteins. Although no direct evidence has been shown for DIP1/2 dimerization, we observed a self-dimerization of DIP1/2 using yeast two-hybrid experiment (data not show). Nevertheless, a dramatic inhibitory effect is only seen with high amounts of DIP1/2 used in transfection experiment (Figure 6A), which suggests that the dimerization of DIP1/2 may affect its activity. More detailed studies are underway to examine this hypothesis.

In summary, both DIP1/2 and DOC-2/DAB2 form a unique protein complex with a negative regulatory activity that modulates the Ras-mediated signal pathway. This complex is operative in basal cells of the prostate and may orchestrate the differentiation and proliferation potential of these cells during prostate regeneration. In contrast, altered expression of any component of this complex may result in abnormal growth and/or the acquired malignant phenotypes of prostate cancer—and perhaps other types of cancer such as ovarian and breast cancer. Further dissection and functional examination of each component in this complex is warranted.

Acknowledgements

We thank Andrew Webb for editing this manuscript, Hana Sharif for valuable project assistance, Dr. Michael White for HA-tagged Ras expression vector, and Dr. Jonathan Cooper for DAB1 cDNA constructs. This work was supported by grants from the National Institute of Digestion, Diabetes, and Kidney (DK-47657), funding to J.T.H. from the Department of Defense (PC970259); and funding to J.D.M. from Gillson Longenbaugh. The GenBank assession number for DIP1/2 is AF236130.

References

1. Mok, S.C., Wong, K-K., Chan, R.K.W., Lau, C., Tsao, S-W., Knapp, R.C., and Berkowitz, R.S. (1994) Molecular cloning of differentially expressed genes in human epithelial ovarian cancer. *Gynecol. Oncol.* **52**, 247-252.

6. Fuzili, Z., Sun, W., Mittellstaedt, S., Cohen, C., and Xu, X.X. (1999) Disabled-2 inactivation is an early step in ovarian tumorigenicity. *Oncogene* **18**, 3104-3113.

3. Schwahn, D.J. and Medina, D. (1998). p96, a MAPK-related protein, is consistently downregulated during mouse mammary carcinogenesis. *Oncogene* 17, 1173-1178.

4. Tseng, C-P. Brent, D.E., Li, Y.-M., Pong, R.-C., and Hsieh, J.-T. (1998) Regulation of rat DOC-2 gene during castration-induced rat ventral prostate degeneration and its growth inhibitory function in human prostatic carcinoma cells. *Endocrinology* **139**, 3542-3553.

5. Fulop,V., Colitti, C.V., Genest, D., Berkowitz, R.S., Yiu, G.K., Ng, S-W., Szepesi, J., and Mok, S.C. (1998) DOC-2/hDab2, a candidate tumor suppressor gene involved in the development of gestational trophoblastic diseases. *Oncogene* **17**, 419-424.

6. Xu, X.-X., Yang, W., Jackowski, S., and Rock, C.O. (1995) Cloning of a novel phosphoprotein regulated by colony-stimulating factor 1 shares a domain with the *Drosophila disabled* gene product. *J. Biol. Chem.* **270**, 14184-14191.

7. Howell, B.W., Hawkes, R., Soriano, P., and Cooper, J.A. (1997) Neuronal position in the developing brain is regulated by mouse *disabled-1*. *Nature* **389**, 733-737.

8. Howell, B.W., Herrick T.M., Hildebrand, J.D., Zhang, Y., and Cooper, J.A. (1997) Dab1 tyrosine phosphoryltion sites relay positional signals during mouse brain development. *Current Biol.* **10**, 877-885.

9. Xu, X.-X., Yi, T., Tang, B., and Lambeth, J.D. (1998) Disabled-2 (Dab2) is an SH3 domain-binding partner of Grb2. *Oncogene* **16**, 1561-1569.

10. Tseng, C.-P., Ely, B.D., Pong, R.-C., Wang, Z., Zhou, J., and Hsieh, J.-T. (1999) The role of DOC-2/DAB2 protein phosphorylation in the inhibition of AP-1 activity. *J. Biol. Chem.* **274**, 31981-31986.

11. Weijerman, P.C., Konig, J.J., Wong, S.T., Niesters, H.G., and Peehl, D.M.. (1994) Lipofection-mediated immortalization of human prostatic epithelial cells of normal and malignant origin using human papillomavirus type 18 DNA. *Cancer Res.* **54**, 5579-5583.

12. Navone, N., Olive M., Ozen, M., Davis, R., Troncoso, P., Tu, S-M., Johnston, D., Pollack, A., Pathak, S., von Eschenbach, A.C., and Logothetis, C.J. (1997) Establishment of two human prostate cancer cell line derived from a single bone metastasis. *Clin. Cancer Res.*,**3**, 2493-2500.

13. Kim, J.H., Liao, D., Lau, L-F., and Huganir, R. (1998) SynGAP: a synaptic RasGAP that associates with the PSD-95/SPA90 protein family. *Neuron* **20**, 683-691.

14. Gillies, R.J., Didier, N., and Denton, M. (1986) Determination of cell number in monolayer culture. *Anal. Biochem.* **159**, 109-113.

15. Kanamaru, H. and Yoshida, O. (1989) Assessment of in vitro lymphokine activated killer (LAK) cell activity against renal cancer cell lines and its suppression by serum factor using crystal violet assay. *Urol. Res.* **17**, 259-264.

16. Yeung, K., Seitz, T., Li, S., Janosh, P., McFerran, B., Kaiser, C., Fee, F., Katsanakis, K.D., Rose, D.W., Mischak, H., Sedivy, J., and Kolch, W. (1999) Suppression of Raf-1 kinase activity and MAP kinase signaling by RKIP. *Nature* **401**, 173-177.

17. Fields, S. and Song, O-K. (1989) A novel genetic system to detect protein-protein interactions. *Nature* **340**, 245-246.

18. Boguski, M.S., and McCormick, F. (1993) Proteins regulating ras and its relatives. *Nature* **366**, 643-654.

19. Feller, S.F., Ren, R. Hanafusa, H., and Baltimore, D. (1994) SH2 and SH3 domains as molecular adhesives: the interactions of Crk and Abl. *Trends Biochem. Sci* **19**, 453-458.

20. Struhl, K. (1989) Helix-turn-helix, zinc-finger, and leucine-zipper motifs for eukaryotic transcriptional regulatory proteins. *Trends Biochem. Sci.* **14**, 137-140.

21. Schheffzek, K., Lautwein, A., Ahmadian, M.R., and Wittinghofer, A. (1996) Crystal structure of the GTPase-activing domain of human p120GAP and impilcations for the interaction with Ras. *Nature* **384**, 591-596.

22. Howell, B.W., Gertler F.B., and Cooper J.A. (1997) Mouse disabled (mDab1): a Src binding protein implicated in neuronal development. *The EMBO J.* **16**, 121-132.

23. Gideon, P., John, J., Frech. M., Lautwein, A., Clark, R., Scheffler, J.E., and Wittinghofer, A. (1992) Mutational and kinetic analyses of the GTPase-activating protein (GAP)-p21 interaction: The C-terminal domain of GAP is not sufficient for full activity. *Mol. Cell. Biol.* **12**, 2050-2056.

24. Morrison, D., Kaplan, D.R., Rapp, U., and Roberts, T.M. (1998) Signal transduction from membrane to cytoplasm growth factors and membrane-bound oncogene products increase Raf-1 phosphorylation and associated protein kinase activity. *Proc. Natl. Acad. Sci. USA.* **85**, 8855-8859.

25. Wu, T.T., Sikes, R.A., Cui, O., Thalmann, G.N., Kao, C., Murphy, C.F., Yang, H., Zhau, H.E., Balian, G., and Chung, L. W. (1998) Establishing human prostate cancer cell xenografts in bone: induction of osteoblastic reaction by prostate-specific

antigen-producing tumors in athymic and SCID/bg mice using LNCaP and lineage-derived sublines. *Int. J. Cancer.* **77**, 877-894.

26. McCormick, F. (1995) Ras-related proteins in signal transduction. *Mol. Reprod. Dev.* **42**, 500-506.

27. Porter, A.C. and Vaillancourt, R.R. (1998) Tyrosine kinase receptor-activated signal transduction pathways which lead to oncogenesis. *Oncogene* **17**, 1343-1352.

28. Abate, C. and Curran, T. (1990) Encounters with Fos and Jun on the road to AP-1. *Semin. Cancer Biol.* **1**, 19-26.

29. Hakak, Y. and Martin, G.S. (1999) Cas mediates transcriptional activation of the serum response element by Src. *Mol. Cell. Biol.* **19**, 6953-6962.

30. Hata, A., Akita, Y., Suzuki, K., and Ohno, S. (1993) Functional divergence of protein kinase C (PKC) family members. PKC gamma differs from PKC alpha and -beta II and nPKC epsilon in its competence to mediate-12-O-tetradecanoyl phorbol 13-acetate (TPA)-responsive transcriptional activation through a TPA-response element. *J. Biol. Chem.* **268**, 9122-9129.

31. Sozeri, O., Vollmer, K., Liyanage, M., Firth, D., Kour, G., Mark, G. E., and Stabel, S. (1992) Activation of the c-Raf protein kinase by protein kinase C phosphorylation. *Oncogene* **7**, 2259-2262.

32. Denhardt, D.T. (1996) Signal-transducing protein phosphorylation cascades mediated by Ras/Rho proteins in the mammalian cell: potential for multiplex signaling. *Biochem. J.* **318**, 729-747.

33. Gumerlock, P.H., Poonamallee, U.R., Meyers, F.J., and deVere White R.W. (1991) Activated ras alleles in human carcinoma of the prostate are rare. *Cancer Res.* **51**, 1632-1637.

34. Pergolizzi, R.G., Kreis, W., Rottach, C., Susin, M., and Broome, J.D. (1993) Mutational status of codons 12 and 13 of the N-and K-ras genes in tissue and cell lines derived from primary and metastatic prostate carcinomas. *Cancer Invest.* **11**, 25-23.

35. Wittinghofer, A. (1998) Signal transduction via Ras. *J. Biol. Chem.* **379**, 933-937.

Figure legends

Figure 1. Schematic display and amino acid sequence analysis of DIP1/2

(A) Diagram of different 5' untranslation sequences between two isoforms of DIP1/2 cDNAs. GAP, GTPase activating protein; PR, proline rich motif; LZ, leucine zipper domain. (B) Three distinct domains of DIP1/2 protein, GAP domain (bold), ten-proline repeats (italic), and a leucine zipper domain (underlined). (C) Multiple sequence alignment of the GAP domain of DIP1/2 with GAP120, *Homo sapiens* neurofibromin (hNF1), Synaptic Ras GAP (SynGAP), *Rattus norvegicus* RasGAP (rn-GAP), and a novel human RasGAP (nGAP). Bold letters indicate the consensus amino acid residues within the Ras GAP domain.

Figure 2. Profile of DIP1/2 mRNA expression in various rat organs and cell lines

(A) Northern blot analysis was performed to detect expression of DIP1/2 mRNA in different organs. (B) Increased expression of DIP1/2 and DOC-2/DAB2 mRNA in degenerated ventral prostate. Total cellular RNA (20 μg) from each organ or cell line were subjected to Northern analysis using ^{32}P-labeled DIP1/2 probe (1 x 10^6 cpm/ml). NbE, prostatic epithelia from Noble rat; NbF, prostatic fibroblasts from Noble rat; VPE, prostatic epithelia from Sprague-Dawley rat; VPF, prostatic fibroblasts from Sprague-Dawley rat; VP, ventral prostate; DLP, dorsolateral prostate; SV, seminal

vesicle; and CG, coagulating gland. The probe made from glyceraldehyde-3-phosphate-dehydrogenase (GAPDH) cDNA was used as an internal control.

Figure 3. Characterization of anti-DIP1/2 polyclonal antibody and determination of DIP1/2 protein levels in rat organs and human prostate cell cultures

(A) *In vitro* translated DIP1/2 protein (5 µl) and rat brain protein extracts (20 µg) were subjected to Western blot analysis probed with anti-DIP1/2 polyclonal antibody. (B) *In vitro* translated DIP1/2 protein was detected by anti-DIP1/2 antibody preincubated with the indicated amount of synthetic peptide. (C) Sixty micrograms of protein from each organ were detected by anti-DIP1/2 polyclonal antibody, p96 monoclonal antibody, or anti-actin antibody. (D) One hundred micrograms of protein were analyzed from degenerated ventral prostate harvested at the indicated time by Western blot with anti-DIP1/2 antibody. (E) Sixty micrograms of cell extract were subjected to Western blot analysis. PrEC, PZ-HPV-7, and SWNPC2 (normal primary prostatic epithelial cells); SWPC1 and SWPC2 (primary prostate cancer cells); TSU-Pr1, LNCaP, C4-2, $MDAPCa_{2a}$, $MDAPCa_{2b}$, (metastatic prostate cancer cell lines).

Figure 4. Direct interaction between DIP1/2 and DOC-2/DAB2 or DAB1

COS cells were cotransfected with different T7-tagged DOC-2/DAB2 constructs and HA-tagged DIP1/2 constructs for 48 hrs. The supernatants were immunoprecipitated with either T7-antibody conjugated agarose beads (A) or HA-antibody plus protein

A/G agarose beads (B). After centrifugation, pellets were subjected to immunoblotting analysis. The levels of protein expression from each transfection were determined by western analysis (C). Cell lysate from rat brain or prostate was incubated overnight with protein A sepharose beads alone, or plus either p96 antibody (Transduction Laboratories) or DIP1/2 antibody at 4 °C. The blots were probed with either p96 antibody or DIP1/2 antibody (D). Cell lysate was prepared from COS cells transfected with each expression vector and subjected to immunoprecipitation then probed with DIP1/2 antibody (E). IP, immunoprecipitation; IB, immunoblotting.

Figure 5. ***In vitro*** **and** ***in vivo*** **RasGAP activity assays**

(A) Kinetics of RasGAP activity of DIP1/2 protein. One microgram of purified GST protein and different amounts of GST-DIP1/2 were incubated with [γ-^{32}P]-GTP bound Ras. At the indicated time, retention of the unhydrolyzed [γ-^{32}P]-GTP was measured by a filter assay. GST: 1 μg (□); GST-DIP1/2: 0.2 μg (◇); 0.4 μg (○); 1.0 μg (△). (B) *In vitro* GAP assay for DIP1/2 mutant. [γ-^{32}P]-GTP bound Ras was incubated separately with 1 μg purified GST, GST-DIP1/2$_m$, and GST-DIP1/2 protein at 25 °C for 10 min. The unhydrolyzed [γ^{32}P]-GTP was assayed by a filter assay. (C) Interruption of Ras and Raf binding by DIP1/2. C4-2 cells transfected with both HA-tagged Ras and DIP1/2 vectors were treated with EGF (100 ng/ml) for 30 min. After incubating, cell supernatants were precipitated with GST-Raf agarose beads, the precipitates were subjected to immunoblotting. The levels of protein expression from

each transfection were determined by western analysis. IP, immunoprecipitation; IB, immunoblotting.

Figure 6. Interaction of DIP1/2 and DOC-2/DAB2 on SRE reporter gene activity

(A) C4-2 cells were co-transfected with SRE reporter gene, β-galactosidase, and DIP1/2 vectors and then treated with EGF (100 ng/ml) for 14 hrs. (B) C4-2 cells were co-transfected with either ΔB or DIP1/2 or in combination with SRE reporter gene and β-galactosidase vectors and treated with TPA (100 ng/ml) for 14 hrs. Cell lysates were determined by both luciferase and β-galactosidase activity assays. Reporter gene activity from each sample was normalized with β-galactosidase activity. Data represent means ± S.D. from three independent experiments. (C) Effect of TPA on interaction of DIP1/2 and DOC-2/DAB2. C4-2 cells were cotransfected with DIP1/2 in combination of either ΔB or ΔB-S^{24}A. Twenty-four hours after transfection, cells were treated with T-medium containing 0.1% FBS, then 24 hours later, cells were incubated with TPA (100 ng/ml) for 40 min. After incubation, cells were washed with PBS and lysed. Immunoprecipitation and Western blot were performed as described in Figure 4.

Figure 7. Growth inhibitory effect of DIP1/2 on prostate cancer cells

Cells were transfected with either pCI-neo or DIP1/2 expression vector. After G418 selecting, two independent clones were isolated and characterized. (A) The selected

transfectants were characterized by Southern blot analysis. (B) Increased protein expression was detected by DIP1/2 antibody. (C) The *in vitro* growth rate for each clone was determined by crystal violet assay. Data represent the mean ± S.D. from six determinants.

Figure 8. Effect of transient transfection of DIP1/2 and DIP/2_m on the growth of prostate cancer cells

(A) C4-2 cells (3 x 10^4) were pleated on 35 mm dish with T-medium containing 5% FBS and co-transfected with 0.2 μg of _-gal expression vector in combination with 0.8 μg pCI-neo (1), DIP1/2_m (2), and DIP1/2 (3) cDNA respectively. Twenty-four hours after transfection, cells were changed to T-medium containing 0.2% FBS. At the indicated time, cells were washed with cold PBS twice and fixed. The number of blue cells was counted by β-gal staining according to Yeung *et al.* (16). (B) At the indicated time, Western blot analysis was used to determine the protein expression of DIP1/2 and DIP1/2_m using DIP1/2 antibody. (C) Actin was used as an internal control for equal protein loading.

Table 1 Effect of DIP1/2 and ΔB on TPA-induced gene activation in prostate cancer

	Relative Luciferase activity [a]	
	Experiment I	Experiment II
PCI-neo	36.1 ± 4.5	33.0 ± 0.2
ΔB	21.8 ± 1.1	13.7 ± 1.9
ΔB-S^{24}A	35.9 ± 0.7	33.1 ± 0.3
DIP1/2	25.1 ± 2.4	12.4 ± 1.2
ΔB +DIP1/2	15.2 ± 1.9	6.3 ± 0.2
ΔB-S^{24}A+DIP1/2	26.7 ± 1.4	11.4 ± 2.1

[a] The relative luciferase gene activity is expressed as folds of induction compared with ethanol control. The results were calculated as mean±S.D. in triplicate

Figure 1

A

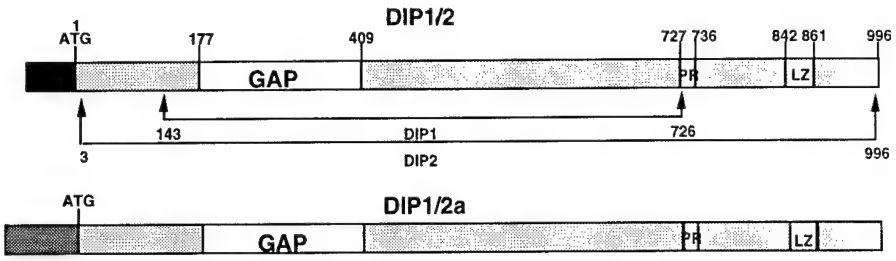

B

```
MENLRRAVHP NKDNSRRVEH ILKLWVIEAK DLPAKKKYLC CLCLDDVLYA  50
RTTGKLKTDN VFWGEHFEFH NLPPLRTVTV HLYRETDKKK KKERNSYLGL  100
VSLPAASVAG RQFVEKWYPV VTPNPKGGKG PGPMIRIKAR YQTITILPME  150
MYKEFAEHIT NHYLGLCAAL EPILSAKTKE EMASALVHIL QSTGKVKDFL  200
TDLMMSEVDR CGDNEHLIFR ENTLATKGIE EYLKLVGHYL LQDALCEFIK  250
ALYESDENCE VDPSKCSAAD LPEHQGNLKM CCELAFCKII NSYCVFPREL  300
KEVFASWRQE CSSRGRPDIS ERLISASLFL RFLCPAIMSP SLFNLLQEYP  350
DDRTARTLTL IAKVTQNLAN FAKFGSKEEY MSFMNQFLEH EWTNMQRFLL  400
EISNPETLSN TAGFEGYIDL GRELSSLHSL LWEAVSQLDQ SIVSKLGPLP  450
RILRDVHTAL STPGSGQLPG TNDLASTPGS GSSSVSTGLQ KMVIENDLSG  500
LIDFTRLPSP TPENKDLFFV TRSSGVQPSP ARSSSYSEAN EPDLQMANGS  550
KSLSMVDLQD ARTLDGEAGS PVGPEALPAD GQVPATQLVA GWPARAAPVS  600
LAGLATVRRA VPTPTTPGTS EGAPGRPQLL APLSFQNPVY QMAAGLPLSP  650
RGLGDSGSEG HSSLSSHSNS EELAAAAKLG SFSTAAEELA RRPGELARRQ  700
MSLTEKGGQP TVPRQNSAGP QRRIDQPPPP PPPPPPAPRG RTPPTMLSTL  750
QYPRPSSGTL ASASPDWAGP GTRLRQQSSS SKGDSPELKP RALHKQGPSP  800
VSPNALDRTA AWLLTMNAQL LEDEGLGPDP PHRDRLRSKE ELSQAEKDLA  850
VLQDKLRIST KKLEEYETLF KCQEETTQKL VLEYQARLEE GEERLRRQQE  900
DKDVQMKGII SRLMSVEEEL KKDHAEMQAA VDSKQKIIDA QEKRIASLDA  950
ANARLMSALT QLKERYSMRA RNGVSPTNPT KLQITENGEF RNSSNC      996
```

C

```
DIP1/2      GKVKDFLTDLMMSEVDR-CGDNEHLIFRENTLATKGIEEYLKLVGHKYLQDA
SynGAP      GKAKDFLSDMAMSEVDRFMERE-HLIFRENTLATKAIEEYMRLIGQKYLKDA
rn-GAP      KLESLLLCTLNDREIS--MEDEATTLFRATTLASTLMEQYMKATATQFVHHA
nGAP        GRAKDFLTDLVMSEVDR-CGEHDVLIFRENTIATKSIEEYLKLVGQQYLHDA
hNF1        HLLYQLLWNMFSKEVE--LADSMQTLFRGNSLASKIMTFCFKVYCATYLQKL
p120GAP     KLESLLLCTLNDREISM--EDEATTLFRATTLASTLMEQYMKATATQFVHHA

DIP1/2      LCEFIKALYESDE-----NCEVDPSKCSAAD-LPEHQGNLKMCCELAFCKII
SynGAP      IGEFIRALYESEE-----NCEVDPIKCTAS-SLAEHQANLRMCCELALCKVV
rn-GAP      LKDSILKIMESKQ-----SCELSPSKLEKNEDVNTNLAHLLSILSELVEKIF
nGAP        LGEFIKALYESDE-----NCEVDPSKCSSSE-LIDHQSNLKMCCELAFCKII
hNF1        L-DPLLRIVITSSDWQHVSFEVDPTRLEPSESLEENQRNLLQMTEKFFHAII
p120GAP     LKDSILKIMESKQ-----SECLSPSKLKKNEDVNTNLTHLLNILSELVEKIF

DIP1/2      NSYCVFPRELKEVFASWRQECSSR--GRPDISERLISASLFLRFLCPAIMSP
SynGAP      NSHCVFPRELKEVFASWRLRCAER--GREDIADRLISASLFLRFLCPAIMSP
rn-GAP      MASEILPPTLRYIYGCLQKSVQHKWPTNNTMRTRVVSGFVFLRLICPAILNP
nGAP        NSYCVFPRELKEVFASWKQQCLNR--GKQDISERLISASLFLRFLCPAIMSP
hNF1        SSSSEFPPQLRSVCHCLYQVVSQRFPQNSIG---AVGSAMFLRFINPAIVSP
p120GAP     MASEILPPTLRYIYGCLQKSVQHKWPTMTTMRTRVVSGFVFLRLICPAILNP

DIP1/2      SLFNLLQEYPDDRTARTLTLIAKVTQNLANFAKFGSKEEYMSFMNQFLEHE-
SynGAP      SLFGLMQEYPDEQTSRTLTLIAKVIQNLANFSKFTSKEDFLGFMNEFLELE-
rn-GAP      RMFNIISDSPSPIAARTLTLVAKSVQNLANLVEFGAKEPYMEGVNPFIKSN-
nGAP        SLFNLMQEYPDDRTSRTLTLIAKVIQNLANFAKFGNKEEYMAFMNDFLEHE-
hNF1        YEAGILDKKPPPRIERGLKLMSKILQSIANHVLF-TKEEHMRPFNDFVKSNF
p120GAP     RMFNIISDSPSPIAARTLILVAKSVQNLANLVEFGAKEPYMEGVNPFIKSN-

DIP1/2      WTNMQRFLLEISNPETLS
SynGAP      WGSMQQFLYEISNLDTLT
rn-GAP      KHRMIMFLDELGNVPELP
nGAP        WGGMKRFLLEISNPDTIS
hNF1        DAARRFFLDIASDCPTSD
p120GAP     KHRMIMFLDELGNVPELP
```

Figure 2

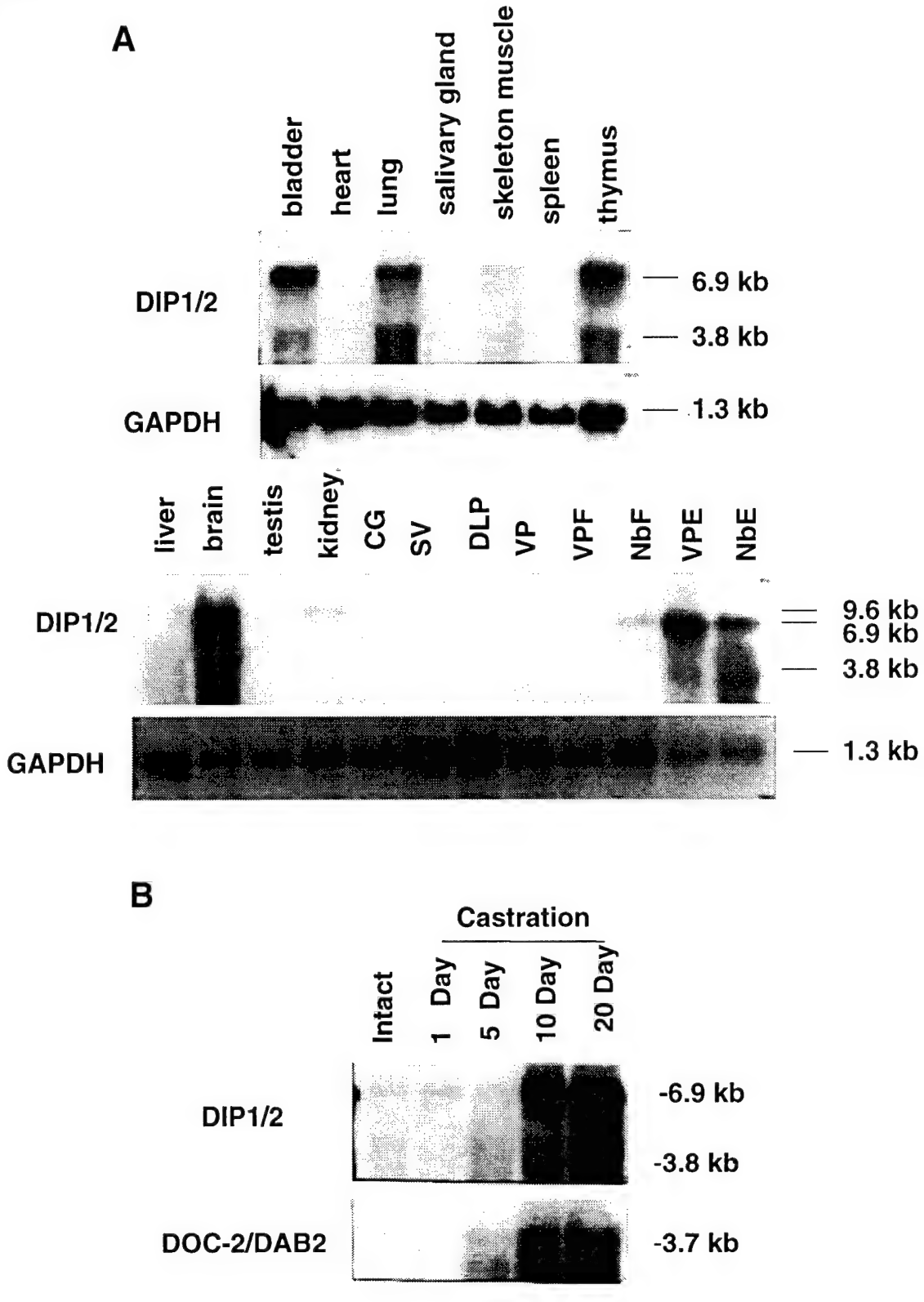
A
bladder
heart
lung
salivary gland
skeleton muscle
spleen
thymus
DIP1/2
6.9 kb
3.8 kb
GAPDH
1.3 kb
liver
brain
testis
kidney
CG
SV
DLP
VP
VPF
NbF
VPE
NbE
DIP1/2
9.6 kb
6.9 kb
3.8 kb
GAPDH
1.3 kb
B
Castration
Intact
1 Day
5 Day
10 Day
20 Day
DIP1/2
-6.9 kb
-3.8 kb
DOC-2/DAB2
-3.7 kb

Figure 3

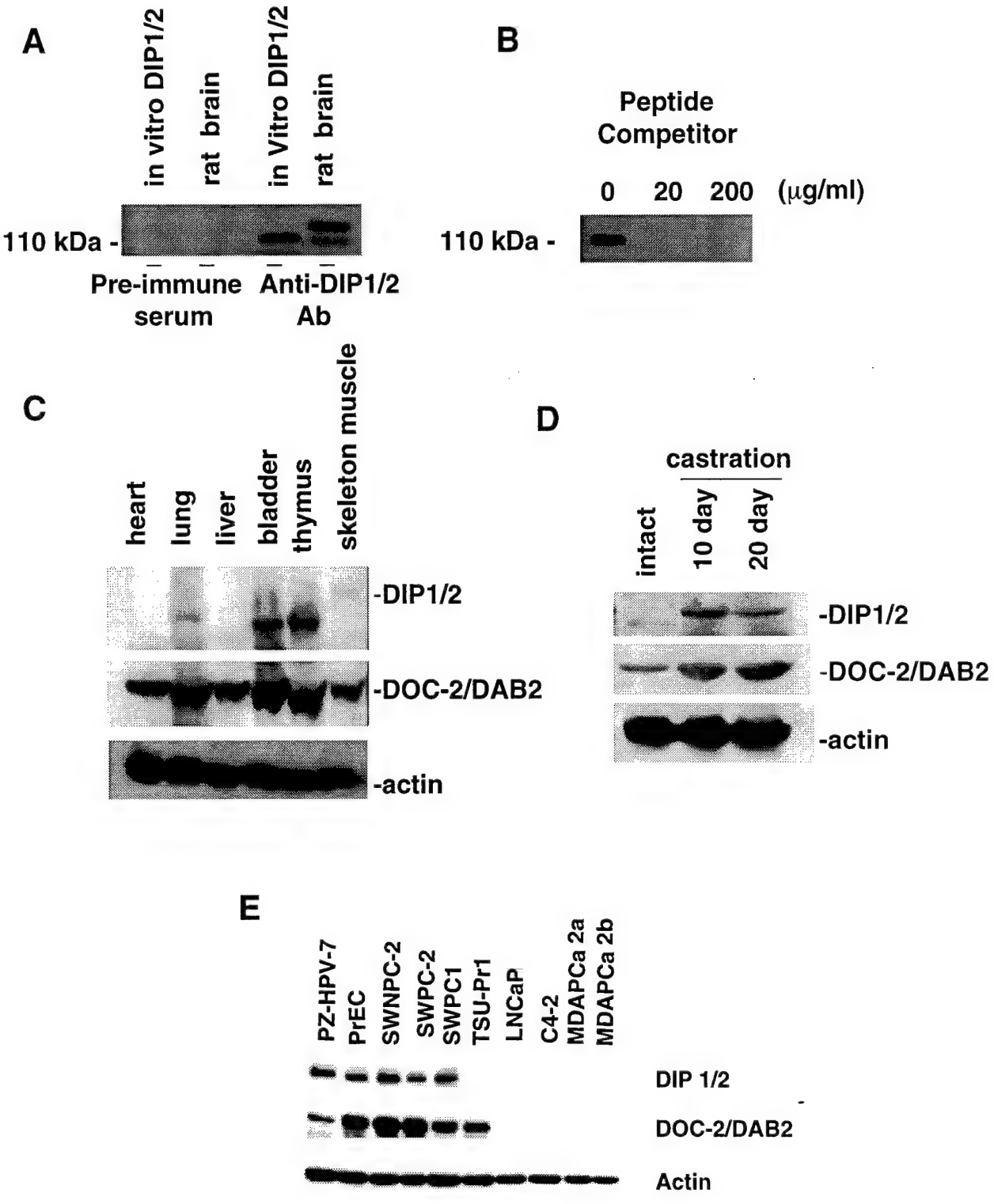
A
in vitro DIP1/2
rat brain
in Vitro DIP1/2
rat brain
110 kDa -
Pre-immune serum
Anti-DIP1/2 Ab
B
Peptide Competitor
0 20 200 (μg/ml)
110 kDa -
C
heart
lung
liver
bladder
thymus
skeleton muscle
-DIP1/2
-DOC-2/DAB2
-actin
D
castration
intact
10 day
20 day
-DIP1/2
-DOC-2/DAB2
-actin
E
PZ-HPV-7
PrEC
SWNPC-2
SWPC-2
SWPC1
TSU-Pr1
LNCaP
C4-2
MDAPCa 2a
MDAPCa 2b
DIP 1/2
DOC-2/DAB2
Actin

Figure 4

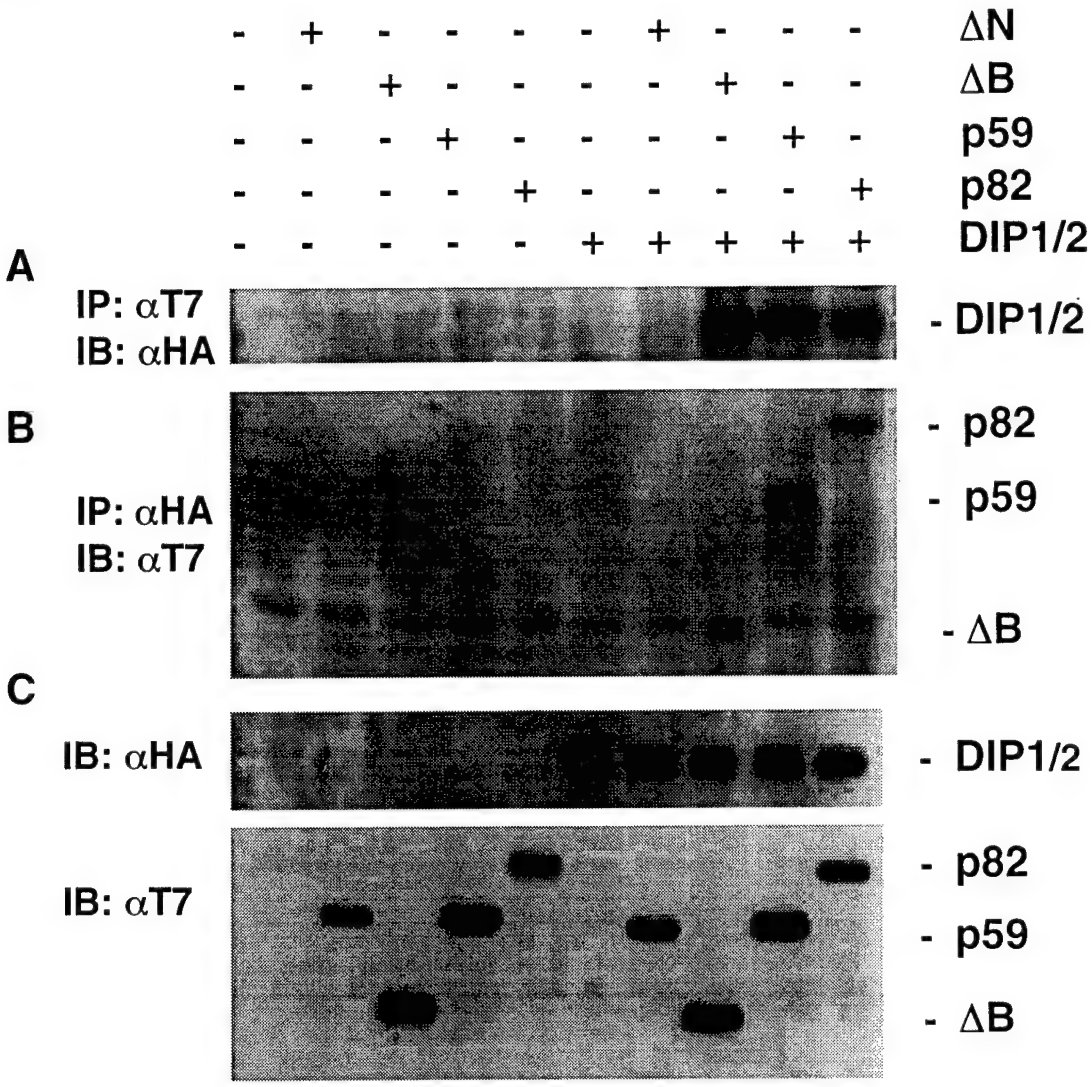
- + - - - - + - - - ΔN
- - + - - - - + - - ΔB
- - - + - - - - + - p59
- - - - + - - - - + p82
- - - - - + + + + + DIP1/2
A
IP: αT7
IB: αHA
- DIP1/2
B
IP: αHA
IB: αT7
- p82
- p59
- ΔB
C
IB: αHA
- DIP1/2
IB: αT7
- p82
- p59
- ΔB

Figure 4

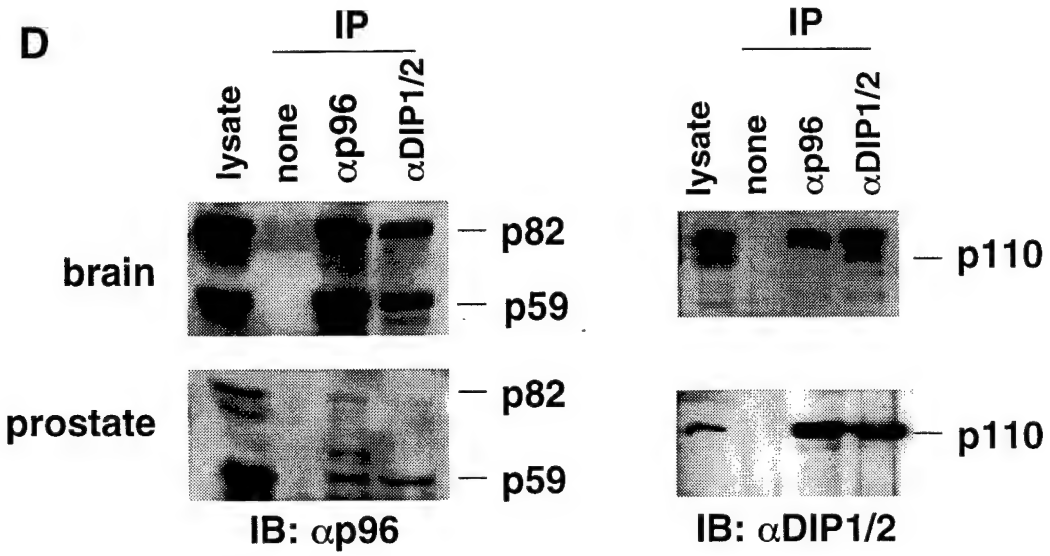
D
IP
lysate
none
αp96
αDIP1/2
brain
prostate
p82
p59
p110
IB: αp96
IB: αDIP1/2

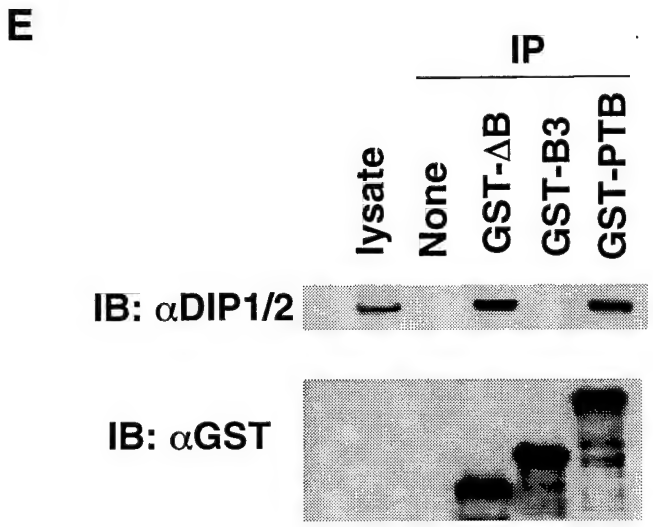
E
IP
lysate
None
GST-ΔB
GST-B3
GST-PTB
IB: αDIP1/2
IB: αGST

Figure 5

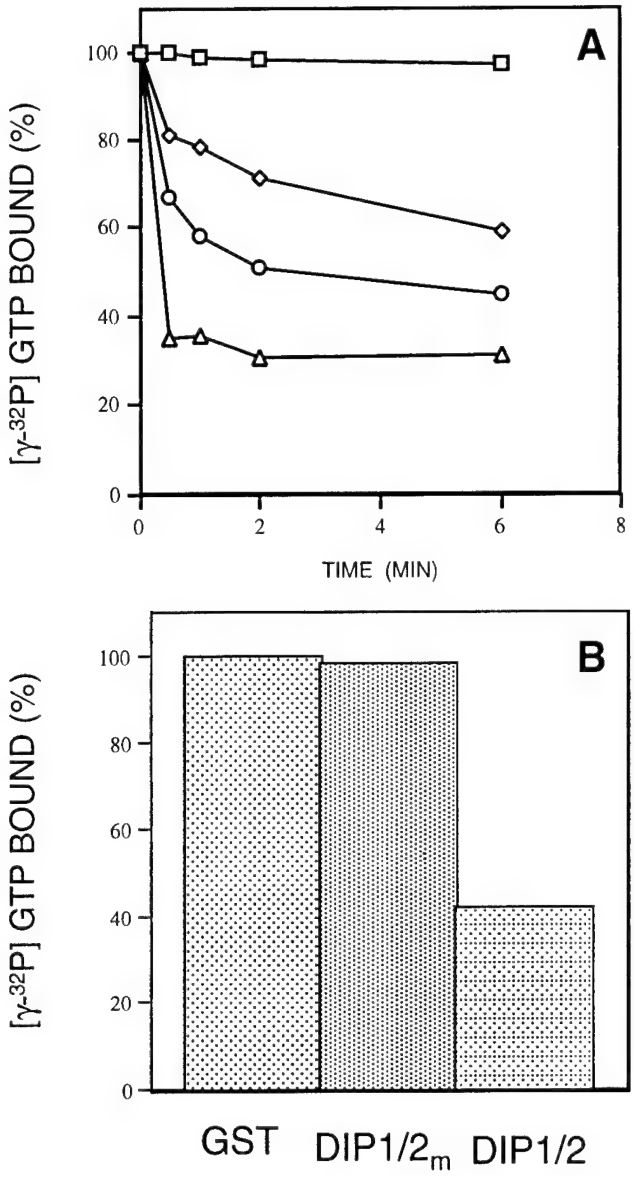
A
100
80
60
40
20
0
0
2
4
6
8
TIME (MIN)
[γ-32P] GTP BOUND (%)
B
100
80
60
40
20
0
[γ-32P] GTP BOUND (%)
GST
DIP1/2m
DIP1/2

C

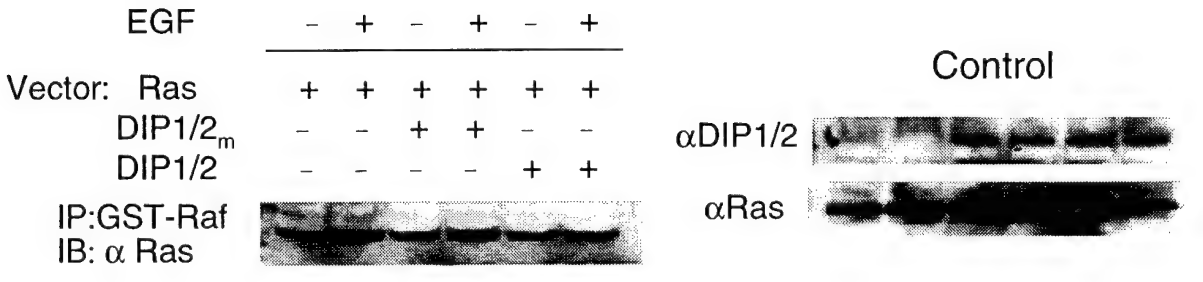
EGF
- + - + - +
Vector: Ras
+ + + + + +
DIP1/2m
- - + + - -
DIP1/2
- - - - + +
IP:GST-Raf
IB: α Ras
Control
αDIP1/2
αRas

Figure 6

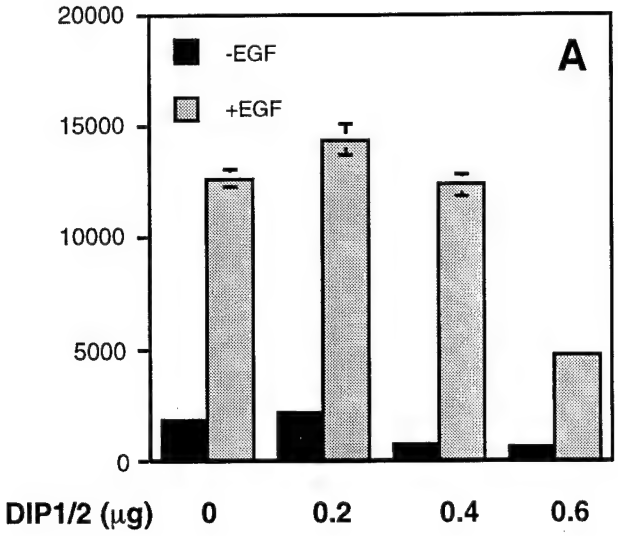
20000
15000
10000
5000
0
-EGF
+EGF
A
DIP1/2 (μg) 0 0.2 0.4 0.6

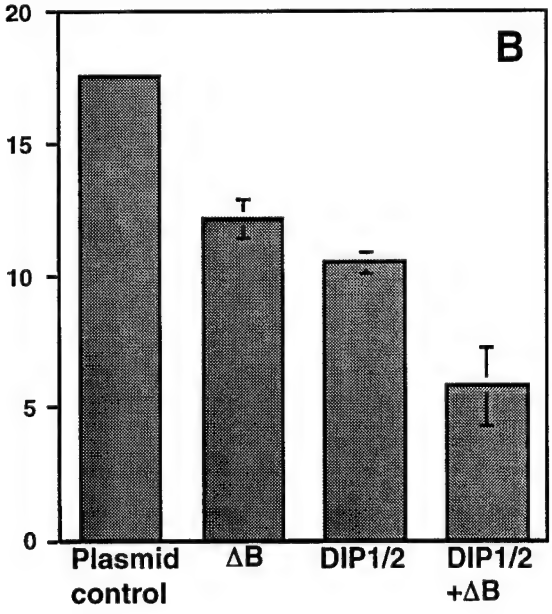
20
15
10
5
0
B
Plasmid control
ΔB
DIP1/2
DIP1/2 +ΔB

C


Control
ΔB
ΔB-S24A
IB: αDIP1/2
TPA - + - +
IP: αT7
IB: αDIP1/2
IB: αT7

Figure 7

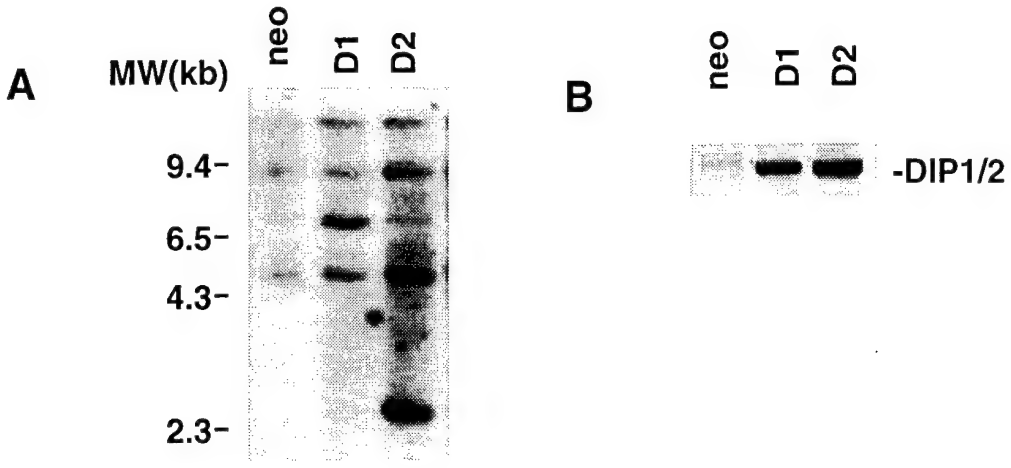
A
MW(kb)
neo
D1
D2
9.4-
6.5-
4.3-
2.3-
B
neo
D1
D2
-DIP1/2

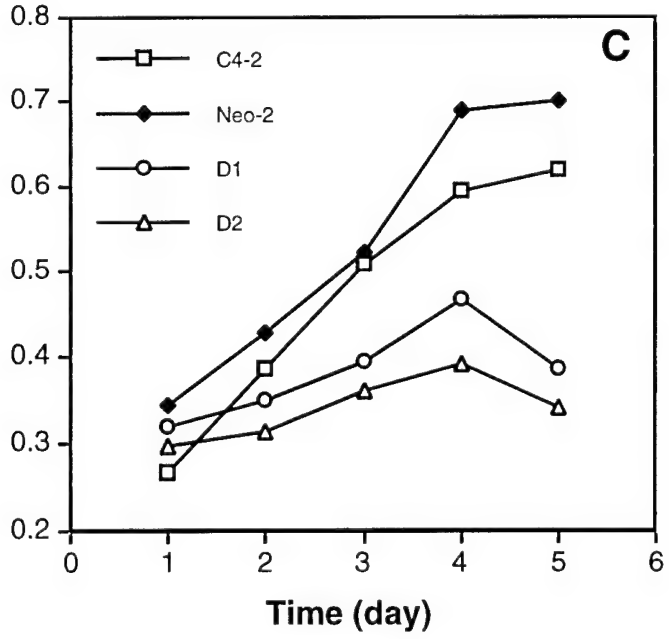
C
C4-2
Neo-2
D1
D2
0.8
0.7
0.6
0.5
0.4
0.3
0.2
0
1
2
3
4
5
6
Time (day)

Figure 8

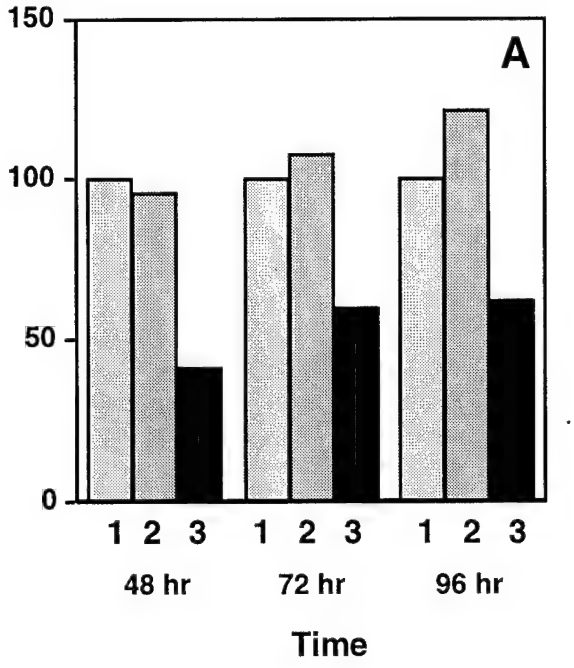
150
100
50
0
A
1 2 3 1 2 3 1 2 3
48 hr
72 hr
96 hr
Time

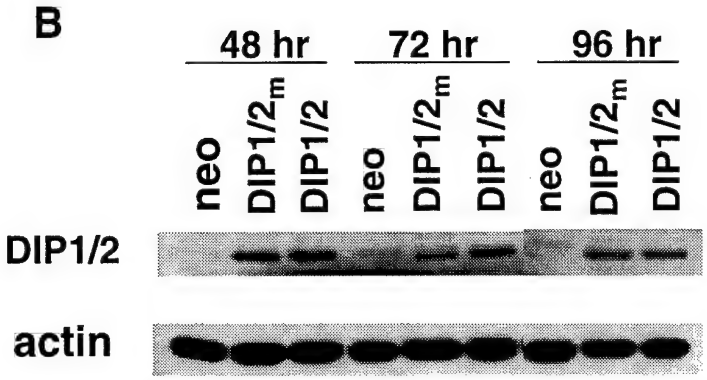
B
48 hr
72 hr
96 hr
neo
DIP1/2m
DIP1/2
DIP1/2
actin

THE JOURNAL OF BIOLOGICAL CHEMISTRY
Vol. 276, No. 30, Issue of July 27, pp. 27793–27798, 2001
Printed in U.S.A.

The Inhibitory Role of DOC-2/DAB2 in Growth Factor Receptor-mediated Signal Cascade

DOC-2/DAB2-MEDIATED INHIBITION OF ERK PHOSPHORYLATION VIA BINDING TO Grb2*

Received for publication, March 29, 2001, and in revised form, May 18, 2001
Published, JBC Papers in Press, May 22, 2001, DOI 10.1074/jbc.M102803200

Jian Zhou and Jer-Tsong Hsieh‡

From the Department of Urology, University of Texas Southwestern Medical Center, Dallas, Texas 75390-9110

DOC-2/DAB2 (differentially expressed in ovarian carcinoma-2/disabled 2) appears to be a potential tumor suppressor gene with a growth inhibitory effect on several cancer types. Previously, we have shown that DOC-2/DAB2 suppresses protein kinase C-induced AP-1 activation, which is modulated by serine 24 phosphorylation in the N terminus of DOC-2/DAB2. However, the functional impact of the C terminus of DOC-2/DAB2, containing three proline-rich domains, has not been explored. In this study, we examined this functional role in modulating signaling mediated by peptide growth factor receptor tyrosine kinase, particularly because it involves the interaction with Grb2. Using sequence-specific peptides, we found that the second proline-rich domain of DOC-2/DAB2 is the key binding site to Grb2 in the presence of growth factors. Such elevated binding interrupts the binding between SOS and Grb2, which consequently suppresses downstream ERK phosphorylation. Reduced ERK phosphorylation was restored when the binding between DOC-2/DAB2 and Grb2 was interrupted by a specific peptide or by increasing the expression of Grb2. Furthermore, the C terminus of the DOC-2/DAB2 construct can inhibit the AP-1 activity elicited by growth factors. We conclude that DOC-2/DAB2, a potent negative regulator, can suppress ERK activation by interrupting the binding between Grb2 and SOS that is elicited by peptide growth factors. This study further illustrates that DOC-2/DAB2 has multiple effects on the RAS-mediated signal cascades active in cancer cells.

DOC-2/DAB2 (differentially expressed in ovarian carcinoma-2/disabled 2) is a potential tumor suppressor associated with ovarian (1), choriocarcinoma (2), prostate (3), and mammary tumors (4). It is a novel phosphorprotein that contains several unique motifs such as the N-terminal disable-like domain and the C-terminal proline-rich SH3[1]-binding domain. The DOC-2/DAB2 gene was first cloned by a differential display polymerase chain reaction, which screened for gene(s) down-regulated in human ovarian cancer but not in their normal counterpart (5). Using the same technique, our laboratory cloned the rat homologue from a degenerated prostate gland. We demonstrated that DOC-2/DAB2 is: (*a*) associated with the basal cells of the prostate; (*b*) involved in the growth and differentiation of prostate epithelia, and (*c*) able to inhibit the growth of cell lines derived from human prostate cancer (3). Similarly, the inhibitory role of DOC-2/DAB2 has also been shown in cell lines of ovarian cancer and choriocarcinoma (1, 2, 6). Taken together, these data indicate that DOC-2/DAB2 is a potent growth inhibitor.

We examined the mechanism(s) of the DOC-2/DAB2-elicited growth inhibitory pathway in prostate cancer cell lines. We found that phosphorylation of DOC-2/DAB2 at the extreme N-terminal region by protein kinase C suppresses AP-1 activity. Specifically, the phosphorylation of serine 24 in the N terminus of DOC-2/DAB2 is the key amino acid residue modulating its inhibitory effect (7). Our recent study revealed that the N terminus of DOC-2/DAB2 interacts with a RAS GTPase-activating protein,[2] which suggests that DOC-2/DAB2 is involved in the RAS-mediated signal pathway.

The C terminus of DOC-2/DAB2, on the other hand, interacts with Grb2, which is an adapter protein critical in bridging signal transduction between the activated protein receptor tyrosine kinase (RPTK) and the RAS-mediated MAP kinase cascade (8, 9). The functional significance of the binding between DOC-2/DAB2 and Grb2 is undefined. Therefore, we investigated this relationship using two RPTK ligands: epidermal growth factor (EGF) and neurotrophin 3 (NT3).

We demonstrated in four different cell lines that RPTK activation increases the binding of DOC-2/DAB2 (particularly the C terminus) to Grb2. This binding further leads to a decrease in the activation of the downstream effector, ERK phosphorylation, and AP-1-mediated gene transcription. Our data illustrate the underlying mechanism of the C terminus of DOC-2/DAB2 in modulating RPTK activation.

EXPERIMENTAL PROCEDURES

Cell Lines, Synthetic Peptides, and Plasmid Constructs—A rat pheochromocytoma cell line (PC12) was grown in Dulbecco's modified Eagle's medium (Life Technologies, Inc.) supplemented with 10% heat-inactivated horse serum (Life Technologies, Inc.), 5% heat-inactivated fetal bovine serum, 100 units/ml penicillin, and 100 units/ml streptomycin. C4-2, NbE, and COS cells were maintained in T medium supplemented with 5% fetal bovine serum (3). Four peptides were synthesized corresponding to the protein sequence of DOC-2/DAB2: PPQ (amino acids 619–627); PPK (amino acids 714–722); PPL (amino acids 663–671); and LLL (amino acids 663–671, the substitution of proline with leucine). All DOC-2/DAB2 cDNA expression constructs,

* This work was supported in part by National Institutes of Health Grant CA 59939, by United States Army Grant PC970259, and by funds from the Gillson Longenbaugh Foundation. The costs of publication of this article were defrayed in part by the payment of page charges. This article must therefore be hereby marked "*advertisement*" in accordance with 18 U.S.C. Section 1734 solely to indicate this fact.

‡ To whom correspondence should be addressed: University of Texas Southwestern Medical Center, Dept. of Urology, 5323 Harry Hines Blvd., Dallas, TX 75390-9110. Tel.: 214-648-3988; Fax: 214-648-8786; E-mail: JT.Hsieh@UTSouthwestern.edu.

[1] The abbreviations used: SH, Src homology; RPTK, receptor protein tyrosine kinase; EGF, epidermal growth factor; EGFR, epidermal growth factor receptor; NT3, neurotrophin 3; ERK, extracellular signal-related protein kinase; MAP, mitogen-activated protein; Grb2, growth receptor binding protein 2.

[2] Z. Wang, C.-P. Tseng, R. C. Pong, H. Chen, J. D. McConnell, and J.-T. Hsieh, manuscript submitted.

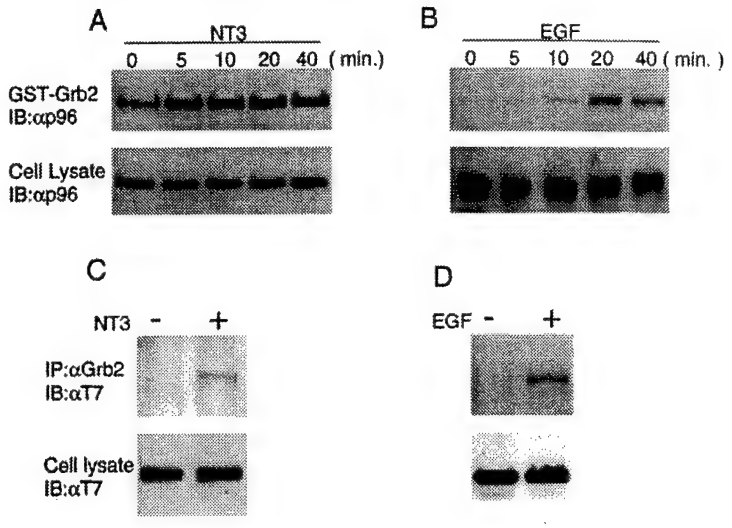

FIG. 1. **The effects of growth factor on the interaction between DOC-2/DAB2 and Grb2.** PC12 (*A*), C4-2 (*B*), and COS (*C* and *D*) cells (6×10^5/60-mm dish) were transfected with 0.6 μg of trkC and 2.4 μg (T7-p82) (*A* and *C*) or 3 μg of p82 (*B* and *D*) for 24 h. After incubating with NT3 (*A* and *C*) or EGF (*B* and *D*), cells were harvested at the indicated time. An aliquot of cell lysate was subjected to a Grb2 binding assay (*A* and *B*) or co-immunoprecipitation (*C* and *D*). In the *upper panels*, the precipitate was probed with anti-DOC-2/DAB2 antibody, αp96 (*A* and *B*) or the anti-T7 tag antibody, αT7 (*C* and *D*). In the *lower panels*, an aliquot of cell lysate was analyzed using Western blot detected by either αp96 (*A* and *B*) or αT7 (*C* and *D*). *IB*, immunoblot.

such as pCI-neo-T7-p82 (T7-p82) and pCI-neo-T7-ΔN (T7-ΔN), have been described (7).

Transfection of Plasmid Vector and Oligopeptide—The indicated number of cells was plated at 37 °C 24 h prior to LipofectAMINE transfection (Life Technologies, Inc.). In each experiment, the control plasmid (pCI-neo) was supplemented to reach an equal amount of total DNA. For the NT3 induction experiment, the trkC expression vector (10), pAC-CMV-trkC, was co-transfected with the DOC-2/DAB2 cDNA construct. 24 h after transfection, cells were switched to a low serum condition (1% heat-inactivated horse serum for PC12 cells; 0.5% fetal bovine serum for COS and C4-2 cells) for another 24 h prior to being treated with growth factors.

For peptide transfection, cells were plated in a 24-well plate with serum-free medium for 24 h. Chariot™ reagent (Active Motif) was mixed with 100 ng of different oligopeptides according to the manufacturer's protocol. 1 h after transfection, cells were treated with growth factors, and cell lysate was prepared at the indicated time.

In Vitro GST-Grb2 Binding Assay—After transfection, cells were exposed to 50 ng/ml of EGF or recombinant NT3 (Upstate Biotechnology). The cells were collected in 0.5 ml of lysis buffer (50 mM Tris-HCl, pH 7.5, 150 mM NaCl, 5 mM EDTA supplemented with 1% of Triton X-100, and a mixture of protease inhibitors) at the indicated time. After a low speed spin, 0.4 ml of supernatant was separately incubated overnight at 4 °C with either 60 μl of GST-Grb2-glutathione Sepharose or GST-glutathione Sepharose. After centrifugation, the pellet was washed twice with the lysis buffer, dissolved in the sample buffer, and then subjected to Western blot analysis probed with either monoclonal antibody against DOC-2/DAB2 (αp96) (Transduction Laboratories) or against the T7 tag (αT7) (Novagen).

Co-immunoprecipitation Assay—The cells were co-transfected with both DOC-2/DAB2 expression vectors and 0.6 μg of Grb2 expression vector (pHM6-Grb2). Using the same treatment protocol, cells were collected in 0.5 ml of lysis buffer. After a low speed spin, 0.4 ml of supernatant was incubated overnight at 4 °C with 1 μg of monoclonal antibody against Grb2 (Transduction Laboratories) and 40 μl of protein G PLUS-agarose (Santa Cruz Biotechnology, Inc.). The pellet was washed twice with lysis buffer, dissolved in sample buffer, and subjected to Western blot analysis detected by the antibody against T7 tag (αT7).

ERK Phosphorylation Assay—Transfected cells were exposed to 50 ng/ml of EGF or NT3 for 10 min and were collected in 70 μl of phosphate-buffered saline (with 1% of Triton X-100 and a mixture of protease inhibitors). After a low speed spin, 20 μl of supernatant was subjected to Western blot analysis. The filter was probed with the antibody against phosphorylated ERK p44/42 (New England Biolab), and the same filter was stripped and reprobed with antibodies against either total ERK 1/2 (p44/42) or p42 (New England Biolab).

Luciferase Reporter Gene Assay—The AP-1-Luciferase reporter construct (−73/+63-Col-Luc) (7) and internal control β-gal vector (pCH110) were used with various DOC-2/DAB2 cDNA expression vectors. The cells were treated with or without 50 ng/ml of EGF or recombinant NT3 for 16 h. Both luciferase and β-galactosidase were assayed (7). The data from the reporter gene activity were normalized with β-galactosidase activity.

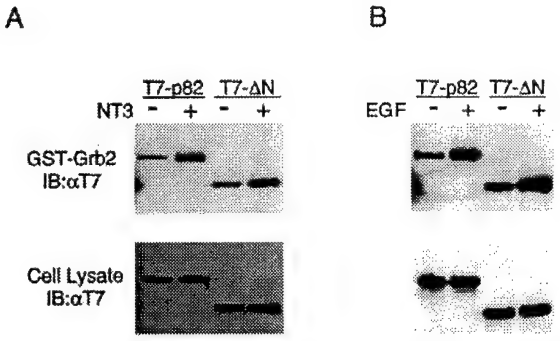

FIG. 2. **The interaction of the C terminus of DOC-2/DAB2 and Grb2.** *A*, COS cells (6×10^5/60-mm dish) were co-transfected with 0.6 μg of pAC-CMV-trkC and 2.4 μg of either DOC-2/DAB2 (T7-p82) or the C terminus of DOC-2/DAB2 (T7-ΔN) and then treated with NT3. *B*, COS cells (6×10^5/60-mm dish) were transfected with 3 μg of either T7-p82 or T7-ΔN and then treated with EGF. Cell lysates were prepared 10 min after treatment and subjected to a Grb2 binding assay. The precipitate (*upper panels*) or total cell lysate (*lower panels*) was detected by anti-T7 tag antibody (*αT7*). *IB*, immunoblot.

RESULTS

NT3 and EGF Increase the Binding of Grb2 to DOC-2/DAB2—In a previous study (7), we showed that the C terminus, but not the N terminus, of DOC-2/DAB2 binds to Grb2. In this study, we investigated the effect of growth factors on this binding. Because DOC-2/DAB2 is expressed in brain tissue (4) and prostate epithelia (3), we chose two RPTK systems: NT3/trkC cascade in PC12 cell and EGF/EGFR cascade in C4-2 cells.

PC12 cells were co-transfected with pAC-CMV-trkC and T7-p82 cDNAs and then treated with NT3 (50 ng/ml) for the indicated time. The cell lysate was prepared and subjected to Grb2-GST binding assay. As shown in the *upper panel* of Fig. 1*A*, a basal level interaction between DOC-2/DAB2 and Grb2 was detected in the PC12 cells; a similar result was shown previously (7). However, binding of DOC-2/DAB2 to Grb2 increased 5 min after treatment with NT3, and increased binding remained constant throughout the entire course of treatment. This indicates that trkC activation can immediately increase the interaction between DOC-2/DAB2 and Grb2. The same expression levels of DOC-2/DAB2 expression were detected in each lane (Fig. 1*A*, *lower panel*), and this rules out the possibility of a transfection artifact.

In the other RPTK signaling system (Fig. 1*B*, *upper panel*),

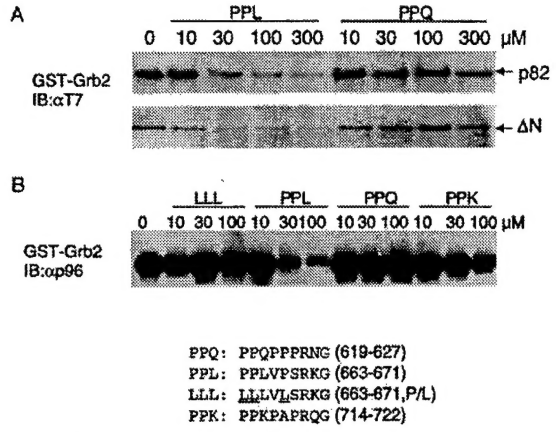

FIG. 3. **The specific interaction of the proline-rich domains in DOC-2/DAB2 and Grb2.** *A*, COS cells (6×10^5/100-mm dish) were transfected with either DOC-2/DAB2 (T7-p82) or the C terminus of DOC-2/DAB2 (T7-ΔN). The cell lysates were prepared 48 h after transfection and subjected to Grb2 binding assay in the presence of different concentrations of oligopeptides. *B*, cell lysate from 80% confluent NbE cells were prepared and subjected to Grb2 binding assay in presence of different concentrations of oligopeptides. The precipitate was detected by either anti-T7 (*αT7*) or anti-p96 (*αp96*) antibodies.

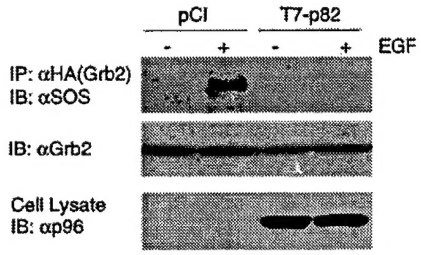

FIG. 4. **The interruption of SOS binding to Grb2 by DOC-2/DAB2.** COS cells (6×10^5/60-mm dish) were co-transfected with HA-Grb2 and either pCI-neo or DOC-2/DAB2 (T7-p82) and then treated with EGF (100 ng/ml) for 10 min. The cell lysates were prepared subjected to co-immunoprecipitation assay by anti-HA tag antibody (*αHA*). The precipitate was detected by anti-SOS antibody (*αSOS*) (*top panel*) and reprobed with anti-Grb2 antibody (*αGrb2*) (*middle panel*). Total cell lysate (*bottom panel*) was detected by anti-p96 antibody (*αp96*). *IB*, immunoblot.

increased binding of DOC-2/DAB2 to Grb2 occurred in a time-dependent manner in a prostatic epithelial cell line (C4-2) treated by EGF. Also, as shown in the *lower panel* of Fig. 1*B*, an equal amount of DOC-2/DAB2 protein expression was detected at each time point. There was difference in the Grb2 binding kinetics between NT3-treated PC12 cells and EGF-treated C4-2 cells. For example, EGF showed a slower rate of Grb2 binding than did NT3. Peak binding of Grb2 occurred 20 min after EGF treatment, compared with 5 min after NT3 treatment. Such difference may influence the effect of DOC-2/DAB2 on the downstream pathway mediated by these two growth factors.

In addition to data obtained from the *in vitro* binding assay, we used co-immunoprecipitation to examine the intracellular interaction between DOC-2/DAB2 and Grb2. As shown in Fig. 1 (*C* and *D*), the complex containing DOC-2/DAB2 significantly increased in the presence of either NT3 or EGF compared with the control. EGF also increased the intracellular interaction between the Grb2 and DOC-2/DAB2. Data from both Grb2 and co-immunoprecipitation assays indicate that the interaction between DOC-2/DAB2 and Grb2 was enhanced under the stimulation of peptide growth factors, which suggests that DOC-2/DAB2 may play a regulatory role in RPTK-mediated signaling.

Growth Factors Enhance the Binding of the C Terminus of DOC-2/DAB2 to Grb2—As we described, the C terminus but not the N terminus of DOC-2/DAB2 interacts with Grb2 (7). To determine whether growth factors increase the affinity of the C terminus of DOC-2/DAB2 to Grb2, we performed Grb2 binding assay using the N-terminal deletion mutant of DOC-2/DAB2 (T7-ΔN). We wanted to validate this interaction using different cell types. Therefore, COS cells were reconstituted with trkC in the presence of either T7-p82 or T7-ΔN construct. As expected, stimulation with NT3 significantly increased the binding of Grb2 to both DOC-2/DAB2 and the C terminus of DOC-2/DAB2 (Fig. 2*A*). This elevated binding was not caused by variable expressions of T7-p82 or T7-ΔN proteins because equal amounts of these proteins were detected. Similarly, Grb2 binding to DOC-2/DAB2 or to the C terminus of DOC-2/DAB2 also increased with EGF treatment (Fig. 2*B*). These data indicate that the binding domain of DOC-2/DAB2 to Grb2 is located in the C terminus of DOC-2/DAB2.

Binding of Grb2 Is Mediated by the Second Proline-rich Domain of DOC-2/DAB2—There are three proline-rich domains in DOC-2/DAB2 with the same consensus sequence as the SOS

FIG. 5. **The suppression of the growth factor-induced ERK phosphorylation mediated by sequestering Grb2 by DOC-2/DAB2 protein.** PC12 (*A* and *C*) and C4-2 (*B* and *D*) cells (8×10^4/12-well plate) were co-transfected with either the control plasmid pCI, full-length (T7-p82), or the C terminus of DOC-2/DAB2 (T7-ΔN) and pAC-CMV-trkC (*A* and *C*) or EGFR expression plasmid (*B* and *D*). In addition, pHM-Grb2 (C, D) was used for increasing Grb2 levels in cells. 24 h after transfection, cells were switched to a low serum medium for another 24 h. 50 ng/ml of NT3 (*A* and *C*) or EGF (*B* and *D*) were added for a 10-min incubation. An aliquot of cell lysate was analyzed by Western blot. In the *upper panels*, the filter was probed with an antibody against phosphorylated ERK p44/42 (αpERK), and in the *lower panels*, the same filter was reprobed with either ERK p42-specific antibody (*αERK2*) or ERK1/2-specific antibody (*αERK1/2*). *IB*, immunoblot.

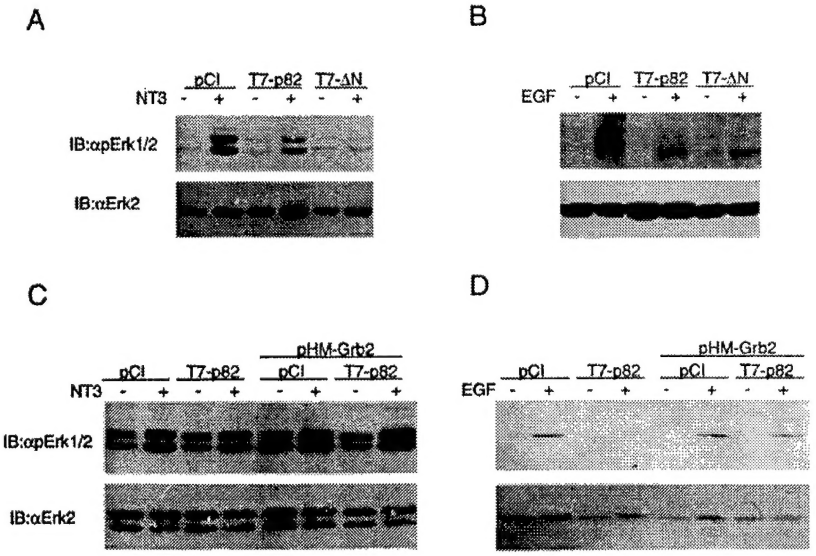

binding site to Grb2. Therefore, all three domains may be involved in Grb2 binding. To compare the binding affinity of these proline-rich sequences, four oligopeptides were synthesized according to the DOC-2/DAB2 protein sequence: PPQ (amino acids 619–627); PPL (amino acids 663–669); LLL (amino acids 663–669 with all proline residues substituted with leucine residues); and PPK (amino acids 714–722). Using the *in vitro* GST-Grb2 binding assay, the PPL peptide blocked the binding of either T7-p82 or T7-ΔN proteins to GST-Grb2, whereas the PPQ peptide had no effect (Fig. 3*A*). Moreover, we prepared cell lysates from NbE cells (a normal rat prostatic epithelial cell line with the endogenous expression of DOC-2/DAB2 proteins) to determine the *in vitro* binding of DOC-2/DAB2 proteins to Grb2. As shown in Fig. 3*B*, PPL effectively blocked the binding in a dose-dependent manner compared with the other two peptides (*i.e.* PPQ and PPK). The effective dose of PPL in COS and NbE cells was very similar, suggesting that the binding kinetics of these proteins remains consistent in different cell lines. The proline residues in this domain are critical for binding because the peptide with leucine substitution (*i.e.* LLL) cannot affect the binding between DOC-2/DAB2 and Grb2 (Fig. 3*B*). These data clearly indicate that the second proline-rich domain in the C terminus of DOC-2/DAB2 is the key interactive site with Grb2.

DOC-2/DAB2 interrupts the binding of Grb2 with SOS Interaction between the Grb2 protein, and the activated receptor can initiate translocation of a group of proteins, namely guanine nucleotide exchange factors (such as SOS), which modulate the GTPase activity of RAS. As shown in Fig. 4, stimulation with EGF increased the binding of Grb2 to SOS in COS cells with no detectable levels of DOC-2/DAB2. However, increased expression of p82 levels in COS cells diminished the binding of Grb2 to SOS, which indicates that DOC-2/DAB2 and SOS compete for the same SH3 site in Grb2.

Both Native DOC-2/DAB2 and the C Terminus of DOC-2/DAB2 Inhibit NT3- and EGF-induced ERK Activation—Grb2 is a key adapter protein for the growth factor-induced MAP kinase pathway (11). To understand the impact of the interaction between DOC-2/DAB2 and Grb2 on this pathway, we examined the phosphorylation status of ERK kinase in the presence of DOC-2/DAB2. Upon the treatment of growth factors, ERK phosphorylation reflected the activation of ERK kinase (12). ERK activation is transient. It peaks at 10 min and then returns to a basal level within 30 min. As shown in Fig. 5*A*, the basal level of phosphorylated ERK was very low in PC12 cells without NT3 treatment. The addition of DOC-2/DAB2 did not alter this level.

In contrast, increasing phosphorylation of ERK1 (44 kDa) and ERK2 (42 kDa) was detected in PC12 cells 10 min after NT3 treatment. Furthermore, NT3-induced phosphorylation of ERK1/2 decreased profoundly in the presence of either full-length DOC-2/DAB2 (T7-p82) or the C terminus of DOC-2/DAB2 (T7- ΔN). Such a change was not caused by the decrease of ERK1/2 protein levels (Fig. 5*A*, *middle* and *lower panel*).

Without EGF treatment, the basal level of ERK2 phosphorylation was lower in C4-2 cells than in PC12 cells (Fig. 5*B*). With EGF treatment, phosphorylation levels of ERK kinases, mainly ERK2 (42 kDa), were elevated. The presence of either T7-p82 or T7-ΔN dramatically suppressed EGF-induced ERK2 phosphorylation. However, the steady-state levels of the ERK2 protein remained the same. These data indicate that ERK2 phosphorylation was inhibited when DOC-2/DAB2 proteins decrease the availability of Grb2 to SOS.

Decreased ERK phosphorylation appears to be a potent downstream event that results from the binding between DOC-2/DAB2 and Grb2. We examined whether increased expression of Grb2 restores the ERK phosphorylation status in cells

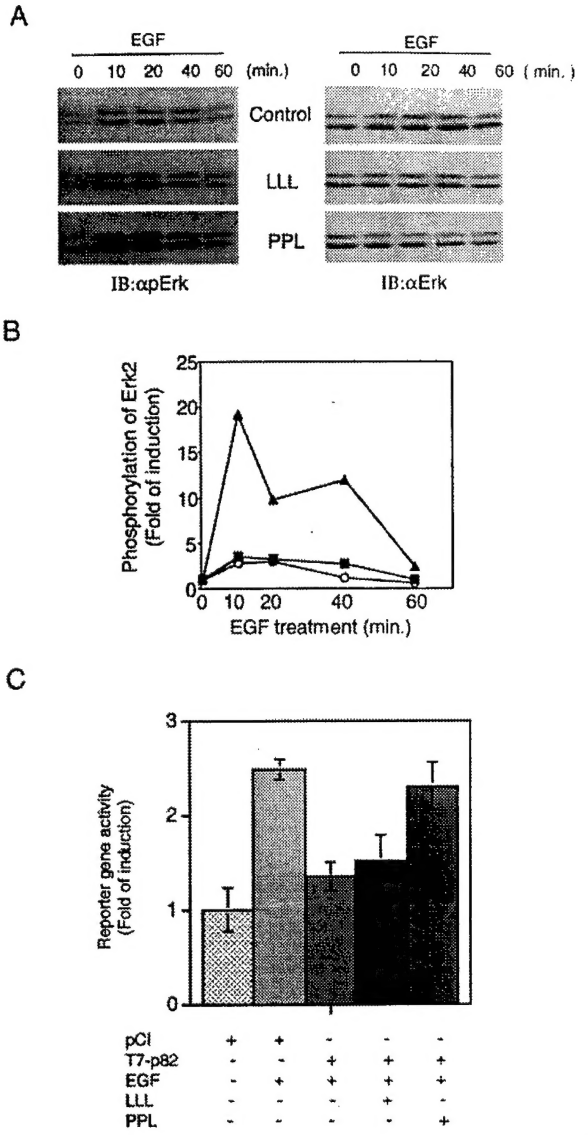

FIG. 6. **The effect of specific peptides derived from DOC-2/DAB2 on EGF-induced ERK phosphorylation.** NbE cells (1×10^4/24 well plate) grew in serum-free medium for 24 h and then were transfected with 100 ng of oligopeptides using Chariot™ reagent. 1 h after transfection, cells were treated with 50 ng of EGF. At the indicated time, cell lysate was prepared and analyzed by Western blot probed with αpERK antibody (*left panels*), and then the same filter was reprobed αERK 1/2 (*right panels*). The intensity of ERK2 signal was determined by densitometer (*A*). The fold of was calculated by normalizing the ratio between phosphorylated ERK2 and total ERK2 proteins induction from each time point with the time 0 (*B*). ○, control; ■, LLL; ▲, PPL. After 16 h of incubation with growth factors, cells were subjected to reporter gene assay (*C*) as described previously (6). *IB*, immunoblot.

treated with growth factors. As shown in Fig. 5 (*C* and *D*), in the absence of either NT3 or EGF, transfection of the Grb2 expression vector failed to induce ERK phosphorylation because Grb2 alone is not capable of activating the growth factor-induced downstream signal pathway (8). In contrast, in either EGF-treated C4-2 or NT3-treated PC12 cells, transfection of the Grb2 expression vector did restore the decreased ERK phosphorylation induced by T7-p82 proteins. This suggests that DOC-2/DAB2 binding to Grb2 is a key step in inactivating ERK phosphorylation.

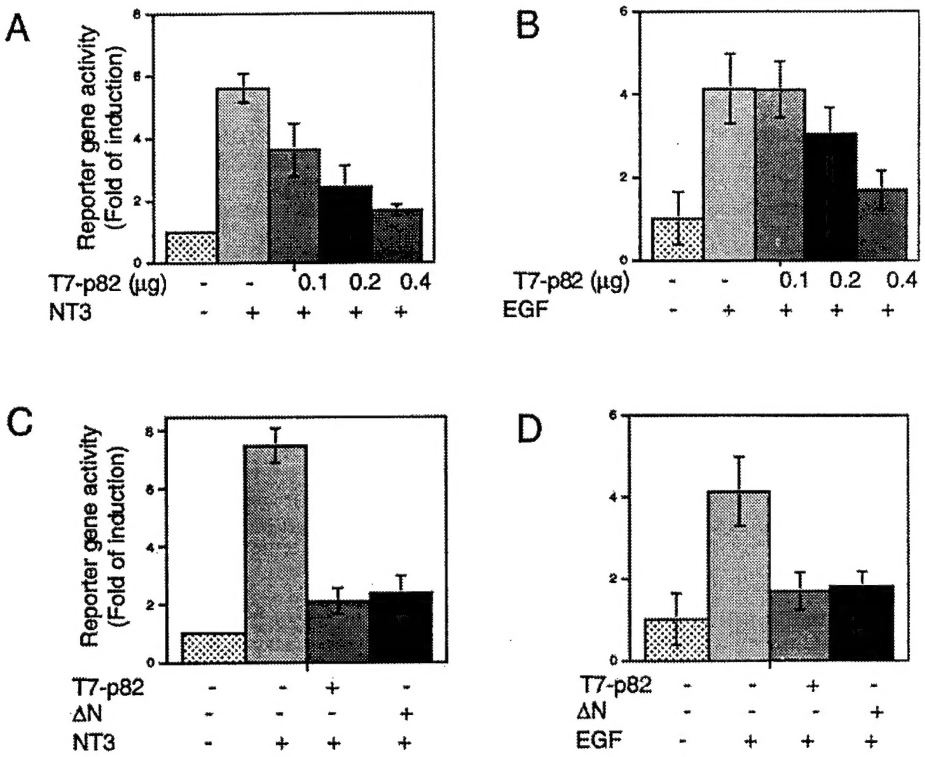

FIG. 7. **The effect of DOC-2/DAB2 and its C-terminal recombinant protein on the growth factor-induced AP-1 activation.** PC12 (*A* and *C*) and C4-2 (*B* and *D*) cells (2×10^5/6-well plate) were co-transfected with 0.2 μg of AP-1 luciferase reporter gene, 0.25 μg of pCH110 (β-gal), and the indicated amount of T7-p82 (*A* and *B*) or 0.4 μg of T7-p82 or T7-ΔN (*C* and *D*). For PC12 cells, 0.15 μg of trkC was included. The total amount of DNA (1 μg/transfection) was supplemented with pCI-neo. 24 h after transfection, cells were down-switched to a low serum for another 24 h. After 16 h of incubation with growth factors, cells were subjected to reporter gene assay. The data represent the means ± S.D. from three independent experiments.

Because the second proline-rich domain of DOC-2/DAB2 is a key binding site to Grb2, we investigated whether blocking this binding also affects the ERK phosphorylation status in cells stimulated with growth factors. To do this, NbE cells were transfected with either PPL or LLL peptide, and the ERK phosphorylation status in EGF-treated NbE cells was determined. As shown in Fig. 6 (*A* and *B*), minutes after EGF treatment, the ERK2 phosphorylation increased about 3–4-fold compared with basal level. PPL enhanced ERK2 phosphorylation about 20-fold. It peaked 10 min after EGF treatment, whereas LLL failed to have the same effect, indicating that PPL can specifically prevent the sequestering Grb2 by the second proline-rich domain of DOC-2/DAB2. These "free" Grb2 molecules amplify signal transduction via the downstream cascade, such as the activation of ERK kinase. Similarly, PPL but not LLL can also antagonize the inhibitory effect of DOC-2/DAB2 on EGF-induced gene transcription (Fig. 6*C*). The overall activity of the reporter gene in this experiment was lower than usual because cell death became more apparent when cells were incubated with both LipofectAMINE and Chariot™ transfection agents. Nevertheless, these data further indicate that one mechanism of DOC-2/DAB2 is to balance the growth factor-induced signal by modulating the availability of effector protein such as Grb2.

Native DOC-2/DAB2 and the C terminus of DOC-2/DAB2 Inhibit NT3- and EGF-induced AP-1 Activation—To determine whether the binding of DOC-2/DAB2 to Grb2 has any impact on RPTK-mediated gene activation, we chose the AP-1 reporter gene assay. AP-1 is activated in PC12 cells upon treatment with neurotrophin (13), and it is the downstream target of RPTK via Grb2 and ERK (14). Suppression on ERK activation indicates that RPTK-induced AP-1 activation may also be affected. As shown in Fig. 7*A*, NT3 induced activation of the AP-1 reporter gene in PC12 cells. In the presence of increasing amounts of T7-p82, the NT3-induced AP-1 activity was suppressed in a dose-dependent manner. In C4-2 cells, the EGF-induced AP-1 activation was also suppressed by T7-p82 in a dose-dependent manner (Fig. 7*B*).

From these results, we believe that the C-terminal recombinant protein has the same inhibitory effect on AP-1 as native DOC-2/DAB2. As depicted in Fig. 7 (*C* and *D*), both T7-p82 and T7-ΔN inhibited NT3- and EGF-induced AP-1 activity with similar magnitude. Thus, the C terminus of DOC-2/DAB2, which contains the Grb2-binding domain(s), is critical to modulate the RPTK-mediated gene expression that is mediated through ERK phosphorylation.

DISCUSSION

Grb2 is a potent adaptor protein. It contains both SH2 and SH3 domains in modulating RPTK-elicited signaling. The SH2 domain directly recognizes phosphotyrosine motifs and is thereby recruited to activated, phosphorylated RPTK. This interaction helps the recruitment of guanine nucleotide exchange factors (*i.e.* SOS) through the binding of the SH3 domain, which subsequently stimulates RAS-GTP binding. The RAS-mediated MAP kinase cascade, a key pathway controlling growth and differentiation, further leads to gene transcription by activating several transcription factors. We and others have shown that DOC-2/DAB2 can interact with Grb2 through its C terminus (7, 15). However, the functional role of this interaction has not been elucidated.

In this study, we manipulated PC12 cell lines without DOC-

2/DAB2 expression such as C4-2 and with different DOC-2/DAB2 cDNA constructs. We found that activation of RPTK by its own ligand also increases the binding of DOC-2/DAB2 to Grb2, which interrupts the binding of SOS to Grb2 (Figs. 1 and 4). We also demonstrated that the second proline-rich domain in the C terminus of DOC-2/DAB2 protein is the key site responsible for the Grb2 binding that prevents a sequential change in the downstream region of the RPTK-mediated pathway (Figs. 3 and 5), including suppressing ERK phosphorylation.

We used a cell line (NbE) that expresses endogenous DOC-2/DAB2 to demonstrate the interaction between endogenous DOC-2/DAB2 and Grb2 proteins. We showed that this interaction appears to be sequence-specific because only peptides with the same sequence as the second proline-rich domain of DOC-2/DAB2 can interrupt Grb2 binding, whereas substitution of key proline residues with leucine residues abolishes its inhibitory function (Fig. 3). Moreover, increasing Grb2 expression in C4-2 cells by using the transient transfection of the Grb2 expression vector alters the inhibitory effect of DOC-2/DAB2 (Fig. 5). We conclude that this inhibitory effect on the MAP kinase pathway results from sequestering Grb2 away from recruiting downstream signaling effectors such as SOS. Therefore, DOC-2/DAB2 represents a potent homeostatic factor that modulates many exogenous stimulus-mediated signal pathways.

To characterize the effect of DOC-2/DAB2 on the RPTK-mediated pathway, we studied two classic ligands in three different cell lines. NT3, which interacts with its receptor trkC, is an important neurotrophin for neuronal development and plasticity. Because other members of the disabled family (*i.e.* DAB1) have been associated with neuronal development (16, 17) and DOC-2/DAB2 is present in brain tissue, we employed PC12 cells (a well established cell model for studying neuronal differentiation) to examine the possible role of DOC-2/DAB2 in NT3-induced signaling. Our results (Figs. 1*A* and 3*A*) demonstrate that DOC-2/DAB2 can block the transient activation of ERK kinase that is considered a mitogenic signal (18) even though neurotrophins can induce a sustained activation of ERK kinase, which can last for several hours in PC12 cells and is related to neuronal differentiation (19). However, we failed to observe any inhibition of the second phase of ERK activation in the presence of DOC-2/DAB2 (data not shown). These results imply that DOC-2/DAB2 may modulate the mitogenic effect of NT3. This function differs from DAB1 protein in neuronal cells.

EGF, a potent mitogen for cell growth, elevation, and EGFR amplification and/or mutation is associated with the progression of many cancer types (20) including prostate cancer (21). Data from our laboratory and others indicate that DOC-2/DAB2 is a tumor suppressor, which is absent in many cancer types (1–6). In this study, we demonstrated that the C terminus of DOC-2/DAB2 may block EGFR-mediated signaling by sequestering Grb2 (Fig. 1) from the upstream of the cascade. This blocking essentially deactivates several key effectors such as ERK and AP-1 (Figs. 3 and 7). Several studies show that unregulated activation of ERK can cause cell transformation (22) and that AP-1 activation is crucial to angiogenesis and neoplastic invasion (23). Moreover, our recent publication indicates that the serine 24 phosphorylation of DOC-2/DAB2 inhibits protein kinase C-mediated gene activation (7). Taken together, we believe that DOC-2/DAB2 represents a unique negative regulator. Upon exogenous stimulus, it demonstrates multiple actions on signaling cascade.

The underlying mechanism regarding the increased affinity of DOC-2/DAB2 to Grb2 by growth factors is still unknown. Our data (Figs. 1 and 2) indicate that this is a rapid event and that the steady-state levels of DOC-2/DAB2 do not change. Therefore, post-translational modification, such as phosphorylation, is likely. Unlike with DAB1 (16), we did not detect any tyrosine phosphorylation in DOC-2/DAB2 (data not shown). Xie *et al.* (24) report that colony-stimulating factor-1 induces serine phosphorylation in DOC-2/DAB2, but they did not determine the key amino acid(s) responsible for this event. We demonstrated that the phorbol ester also induces serine phosphorylation in the N terminus but not in the C terminus of DOC-2/DAB2 (7). Therefore, post-translational modification of DOC-2/DAB2 may play a role in this event because there are several potential ERK phosphorylation sites in the C terminus of DOC2/DAB2 (24). Alternatively, however, we cannot rule out that the presence of other factor(s) may facilitate this interaction upon stimulation with growth factors. Therefore, more detailed study is warranted.

Acknowledgments—We thank Jessica Scholes for excellent technical assistance, Andrew Webb for editorial assistance, and Dr. Koeneman for reading this manuscript.

REFERENCES

1. Mok, S. C., Chan, W. Y., Wong, K. K., Cheung, K. K., Lau, C. C., Ng, S. W., Baldini, A., Colitti, C. V., Rock, C. O., and Berkowitz, R. S. (1998) *Oncogene* **16,** 2381–2387
2. Fulop, V., Colitti, C. V., Genest, D., Berkowitz, R. S., Yiu, G. K., Ng, S.-W., Szepesi, J., and Mok, S. C. (1998) *Oncogene* **17,** 419–424
3. Tseng, C.-P., Ely, B. D., Li, Y., Pong, R.-C., and Hsieh, J.-T. (1998) *Endocrinology* **139,** 3542–3553
4. Schwahn, D. J., and Medina, D. (1998) *Oncogene* **17,** 1171–1178
5. Mok, S. C., Wong, K.-K., Chan, R. K. W., Lau, C. C., Tsao, S.-W., Knapp, R. C., and Berkowitz, R. S. (1994) *Gynecol. Oncol.* **52,** 247–252
6. Fazili, Z., Sun, W., Mittelstaedt, S., Cohen, C., and Xu, X.-X. (1999) *Oncogene* **18,** 3104–3113
7. Tseng, C.-P., Ely, B. D., Pong, R.-C., Wang, Z., Zhou, J., and Hsieh, J.-T. (1999) *J. Biol. Chem.* **274,** 31981–31986
8. Lowenstein, E. J., Daly, R. J., Batzer, A. G., Li, W., Margolis, B., Lammers, R., Ullrich, A., Skolnik, E. Y., Bar-Sagi, D., and Schlessinger, J. (1992) *Cell* **70,** 432–442
9. Margolis, B. (1994) *Prog. Biophys. Mol. Biol.* **62,** 223–244
10. Tsoulfas, P., Soppet, D., Escandon, E., Tessarollo, L., Mendoza-Ramirez, J. L., Rosenthal, A., Nickolics, K., and Parada, L. F. (1993) *Neuron* **10,** 975–990
11. Cobb, M. H. (1999) *Prog. Biophys. Mol. Biol.* **71,** 479–500
12. Robbins, D. J., Cheng, M., Zhen, E., Vanderbilt, C. A., Feig, L. A., and Cobb, M. H. (1992) *Proc. Natl. Acad. Sci. U. S. A.* **89,** 6924–6928
13. Gutacker, C., Klock, G., Diel, P., and Koch-Brandt, C. (1999) *Biochem. J.* **339,** 759–766
14. Karin, M. (1995) *J. Biol. Chem.* **270,** 16483–16486
15. Xu, X.-X., Yi, T., Tang, B., and Lambeth, J. D. (1998) *Oncogene* **16,** 1561–1569
16. Howell, B. W., Gertler, F. B., and Cooper, J. A. (1997) *EMBO J.* **16,** 121–132
17. Howell, B. W., Hawkes, R., Soriano, P., and Cooper, J. A. (1997) *Nature* **389,** 733–737
18. Marshall, C. J. (1995) *Cell* **80,** 179–185
19. York, R. D., Yao, H., Dillon, T., Ellig, C. L., Eckert, S. P., McCleskey, E. W., and Stork, P. J. S. (1998) *Nature* **392,** 622–626
20. Khazaie, K., Schirrmacher, V., and Lichtner, R. B. (1993) *Cancer Metastasis Rev.* **12,** 255–274
21. Ware, J. L. (1998) *Cancer Metastasis Rev.* **17,** 443–447
22. Robinson, M. J., Stippec, S. A., Goldsmith, E., White, M. A., and Cobb, M. H. (1998) *Curr. Biol.* **8,** 1141–1150
23. McCarty, M. F. (1998) *Med. Hypotheses* **50,** 511–514
24. Xu, X.-X., Yang, W., Jackowski, S., and Rock, C. O. (1995) *J. Biol. Chem.* **270,** 14184–14191